Biometrics 59, 1–4 DOI: 000
December 2014

Web-based Supplementary Materials for Multilevel Quantile Function Modeling with Application to Birth Outcomes by Luke B. Smith, Brian J. Reich, Amy H. Herring, Peter H. Langlois, and Montserrat Fuentes.

This paper has been submitted for consideration for publication in *Biometrics*

Web Appendix A

In this section we show the conditional posteriors for our MCMC algorithm. Posterior distributions of θ_{mjg} were updated singly via random walk Metropolis using Gaussian candidate distributions with variances tuned to have acceptance probability between 30 and 40%. Posterior distributions of the autocorrelation parameters ρ_{mj} and range parameters ϕ_{mj} were updated using independent Metropolis updates. The basis function means μ_{mj} were given Gaussian priors with mean μ_0 and precision δ_0. The basis function precisions γ_{mj} were given Gamma priors with shape parameter a and scale parameters b. These means and precisions have conjugate posteriors and were updated using Gibbs sampling.

$$\mu_{mj}|rest \sim N\left(\frac{\gamma_{mj}\mathbf{1^T\Sigma_{mj}^{-1}}\theta_{\mathbf{mj}}}{\gamma_{mj}\mathbf{1^T\Sigma_{mj}^{-1}1}+\delta_{\mathbf{0}}}, (\gamma_{mj}\mathbf{1^T\Sigma_{mj}^{-1}1})^{-1}\right)$$

$$\gamma_{mj}|rest \sim Gamma(G/2+a, (0.5(\theta_{mj}-\mathbf{1}\mu_{\mathbf{mj}})\mathbf{\Sigma_{mj}^{-1}}(\theta_{\mathbf{mj}}-\mathbf{1}\mu_{\mathbf{mj}})+\mathbf{1/b})^{-1})$$

where $\theta_{\mathbf{mj}} = \theta_{\mathbf{mj1}}, ..., \theta_{\mathbf{mjG}}$.

Web Appendix B

In this section we present further simulation study results across different numbers of basis functions.

[Figure 1 about here.]

[Figure 2 about here.]

[Figure 3 about here.]

[Figure 4 about here.]

[Figure 5 about here.]

[Figure 6 about here.]

[Figure 7 about here.]

[Figure 8 about here.]

[Figure 9 about here.]

[Figure 10 about here.]

[Figure 11 about here.]

[Figure 12 about here.]

[Figure 13 about here.]

[Figure 14 about here.]

[Figure 15 about here.]

Web Appendix C

In this section we present evidence of convergence of MCMC chains for the birth outcome analysis.

[Figure 16 about here.]

[Figure 17 about here.]

Web Appendix D

In this section we show plots of regression effects that change across predictor, quantile level, Public Health Region, and gestational age.

[Figure 18 about here.]

[Figure 19 about here.]

[Figure 20 about here.]

[Figure 21 about here.]

[Figure 22 about here.]

[Figure 23 about here.]

[Figure 24 about here.]

[Figure 25 about here.]

[Figure 26 about here.]

[Figure 27 about here.]

[Figure 28 about here.]

[Figure 29 about here.]

[Figure 30 about here.]

[Figure 31 about here.]

[Figure 32 about here.]

[Figure 33 about here.]

[Figure 34 about here.]

[Figure 35 about here.]

[Figure 36 about here.]

[Figure 37 about here.]

[Figure 38 about here.]

[Figure 39 about here.]

[Figure 40 about here.]

[Figure 41 about here.]

[Figure 42 about here.]

[Figure 43 about here.]

[Figure 44 about here.]

[Figure 45 about here.]

[Figure 46 about here.]

[Figure 47 about here.]

[Figure 48 about here.]

[Figure 49 about here.]

[Figure 50 about here.]

[Figure 51 about here.]

[Figure 52 about here.]

[Figure 53 about here.]

[Figure 54 about here.]

[Figure 55 about here.]

[Figure 56 about here.]

[Figure 57 about here.]

[Figure 58 about here.]

[Figure 59 about here.]

Received October 2013.

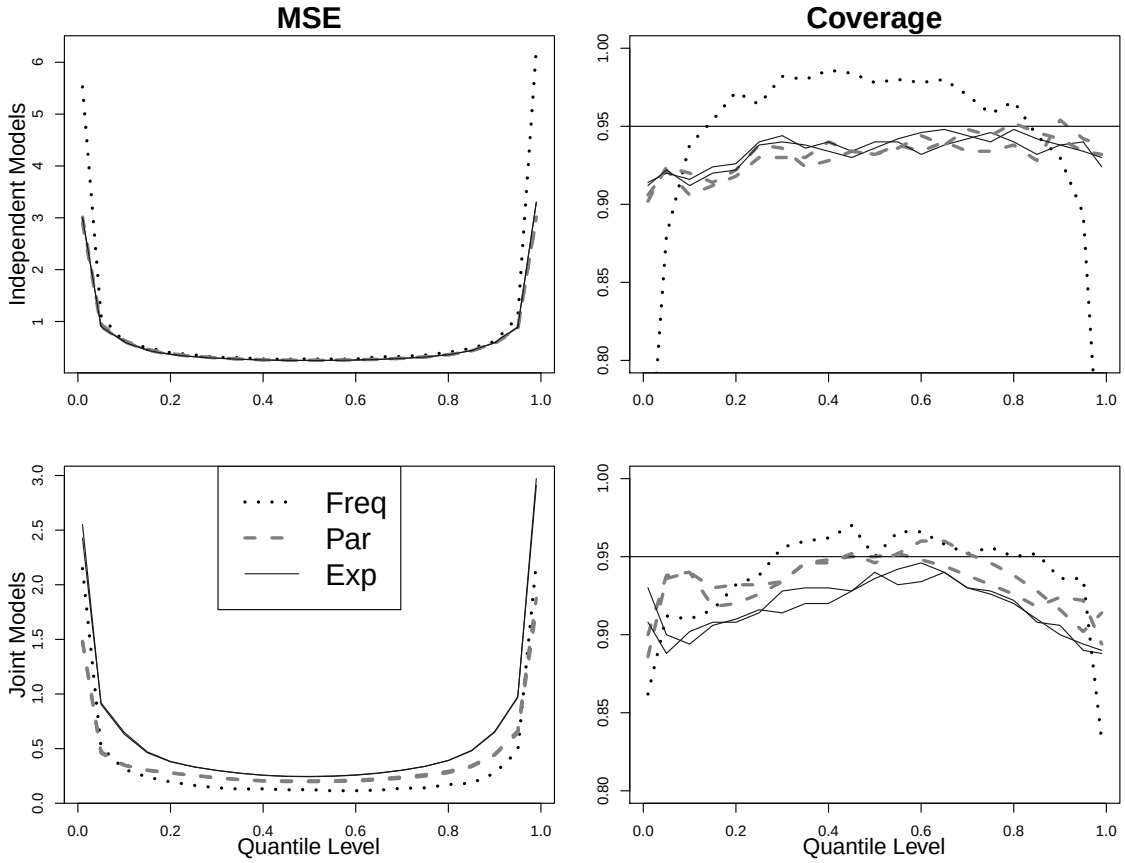

Figure 1. MSE and coverage probabilities for t-distributed response where n = 400 at each gestational age and M was selected by log pseudo marginal likelihood. Results above are for the classical frequentist estimator, spline estimator with Pareto tails, and spline estimator with exponential tails, titled "Freq", "Par", and "Exp" respectively. The maximum Monte Carlo standard error of MSE was 0.02 for Bayesian estimators and 0.13 for the frequentist estimator.

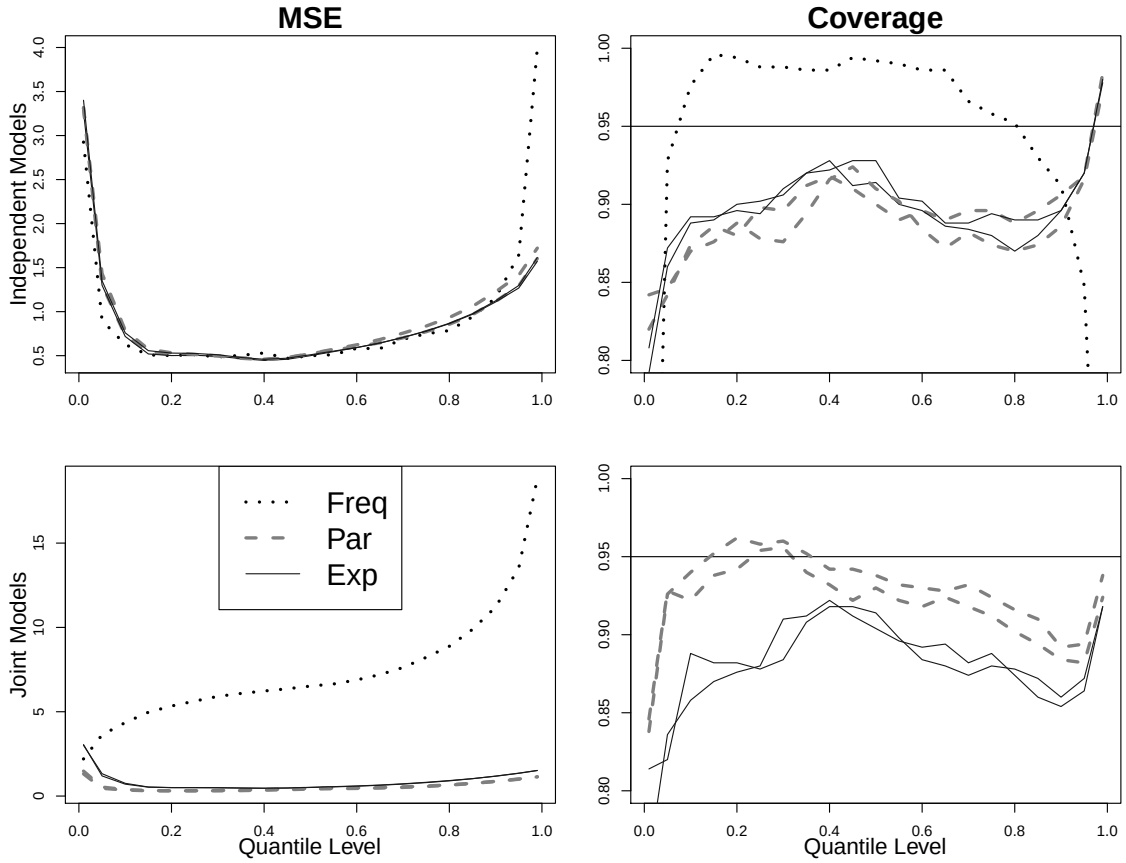

Figure 2. MSE and coverage probabilities for beta-distributed response where n = 200 at each gestational age and M was selected by log pseudo marginal likelihood. Results above are for the classical frequentist estimator, spline estimator with Pareto tails, and spline estimator with exponential tails, titled "Freq", "Par", and "Exp" respectively. The maximum Monte Carlo standard error of MSE was 0.52 for Bayesian estimators and 0.33 for the frequentist estimator.

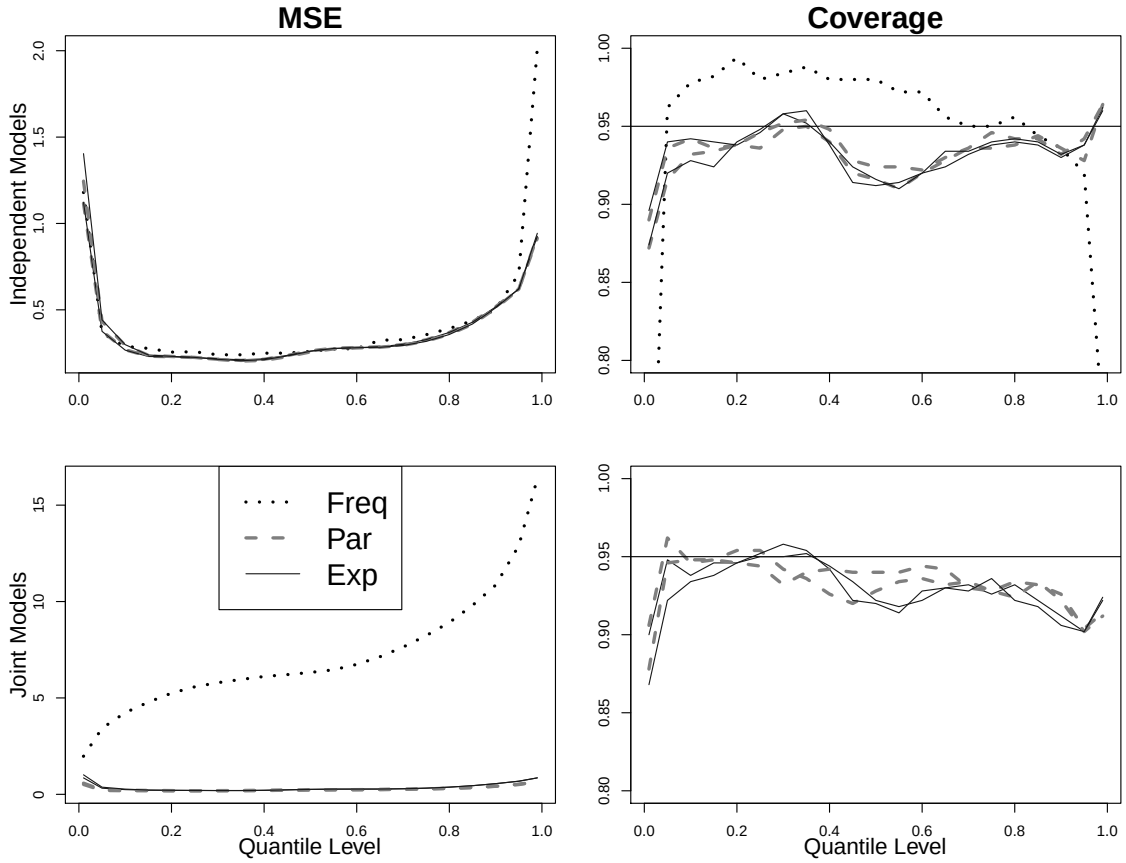

Figure 3. MSE and coverage probabilities for beta-distributed response where n = 400 at each gestational age and M was selected by log pseudo marginal likelihood. Results above are for the classical frequentist estimator, spline estimator with Pareto tails, and spline estimator with exponential tails, titled "Freq", "Par", and "Exp" respectively. The maximum Monte Carlo standard error of MSE was 0.52 for Bayesian estimators and 0.31 for the frequentist estimator.

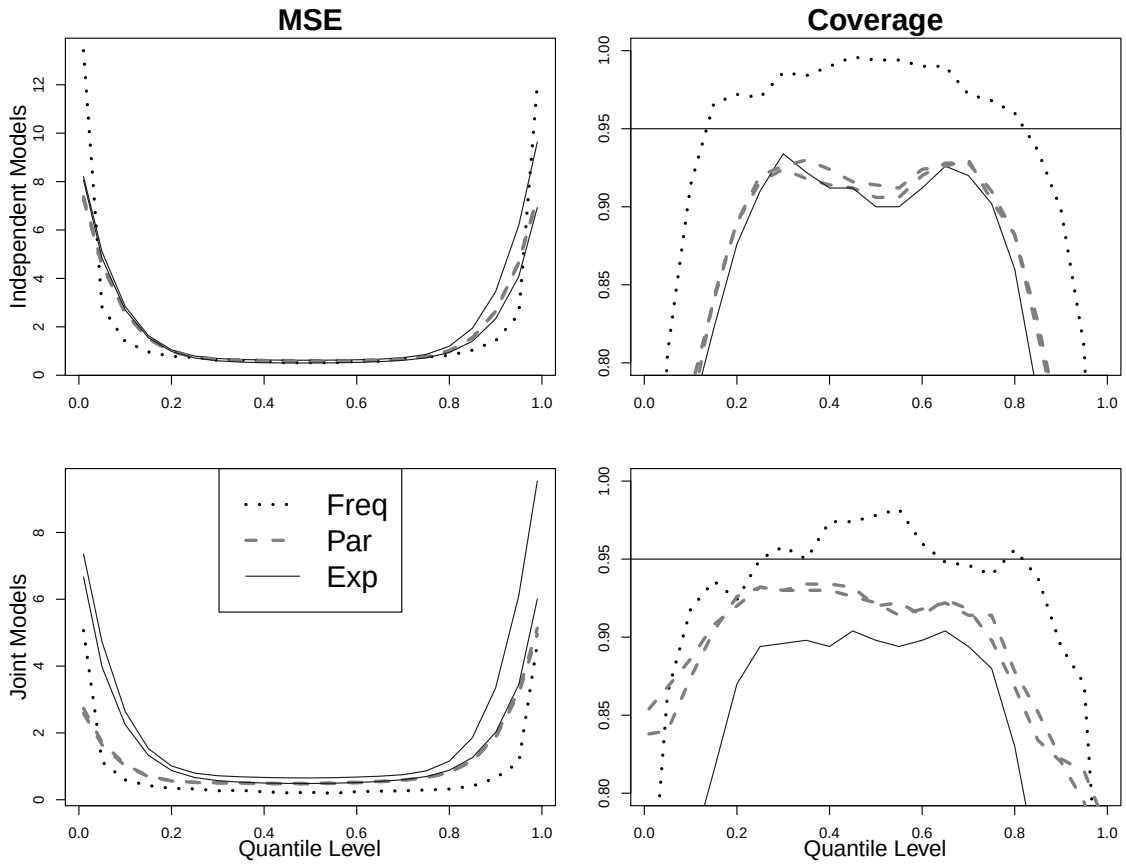

Figure 4. MSE and coverage probabilities for t-distributed response where n = 200 at each gestational age and M = 5. Results above are for the classical frequentist estimator, spline estimator with Pareto tails, and spline estimator with exponential tails, titled "Freq", "Par", and "Exp" respectively.

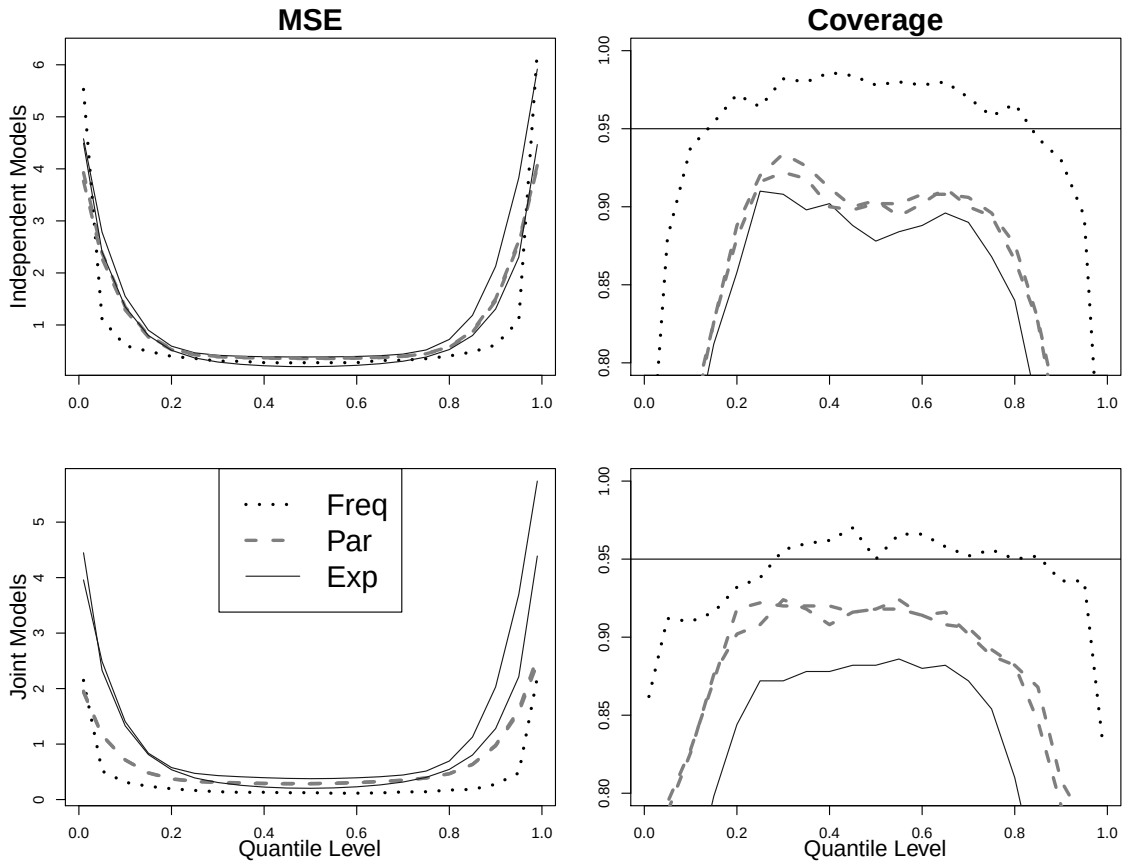

Figure 5. MSE and coverage probabilities for t-distributed response where n = 400 at each gestational age and M = 5. Results above are for the classical frequentist estimator, spline estimator with Pareto tails, and spline estimator with exponential tails, titled "Freq", "Par", and "Exp" respectively.

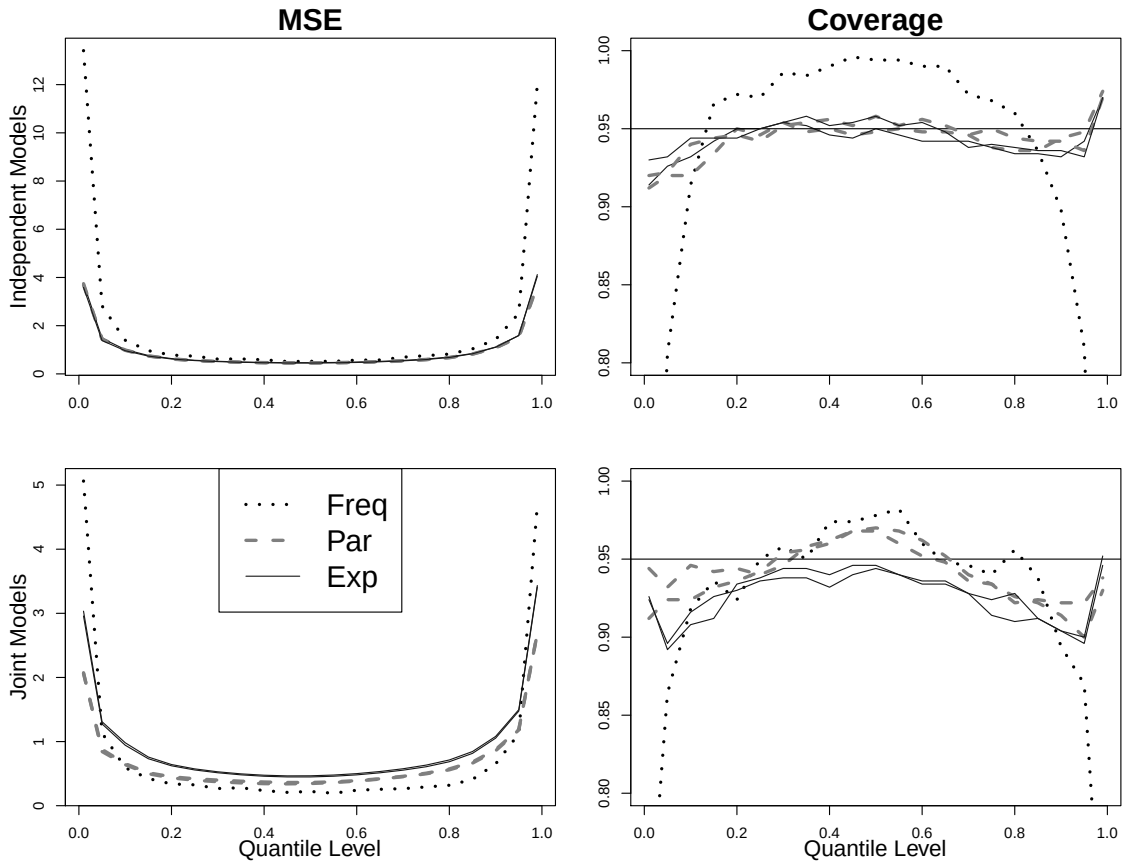

Figure 6. MSE and coverage probabilities for t-distributed response where n = 200 at each gestational age and M = 7. Results above are for the classical frequentist estimator, spline estimator with Pareto tails, and spline estimator with exponential tails, titled "Freq", "Par", and "Exp" respectively.

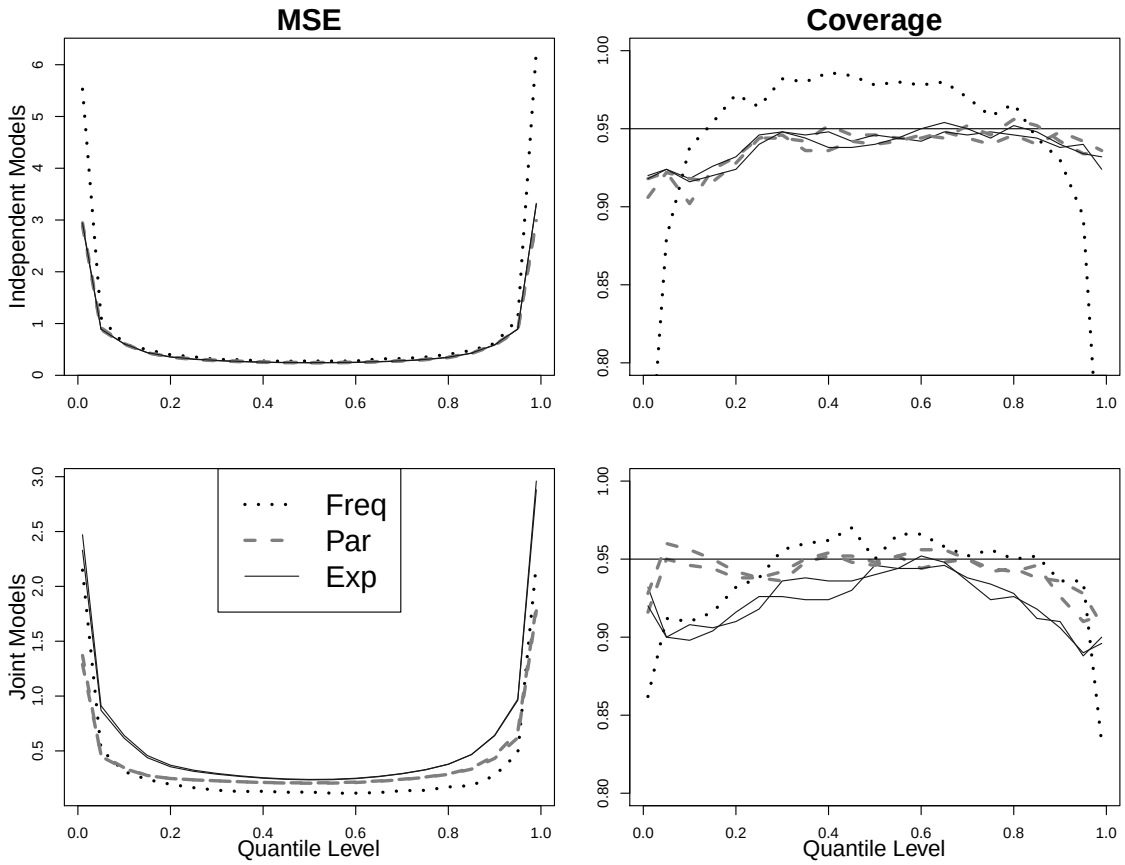

Figure 7. MSE and coverage probabilities for t-distributed response where n = 400 at each gestational age and M = 7. Results above are for the classical frequentist estimator, spline estimator with Pareto tails, and spline estimator with exponential tails, titled "Freq", "Par", and "Exp" respectively.

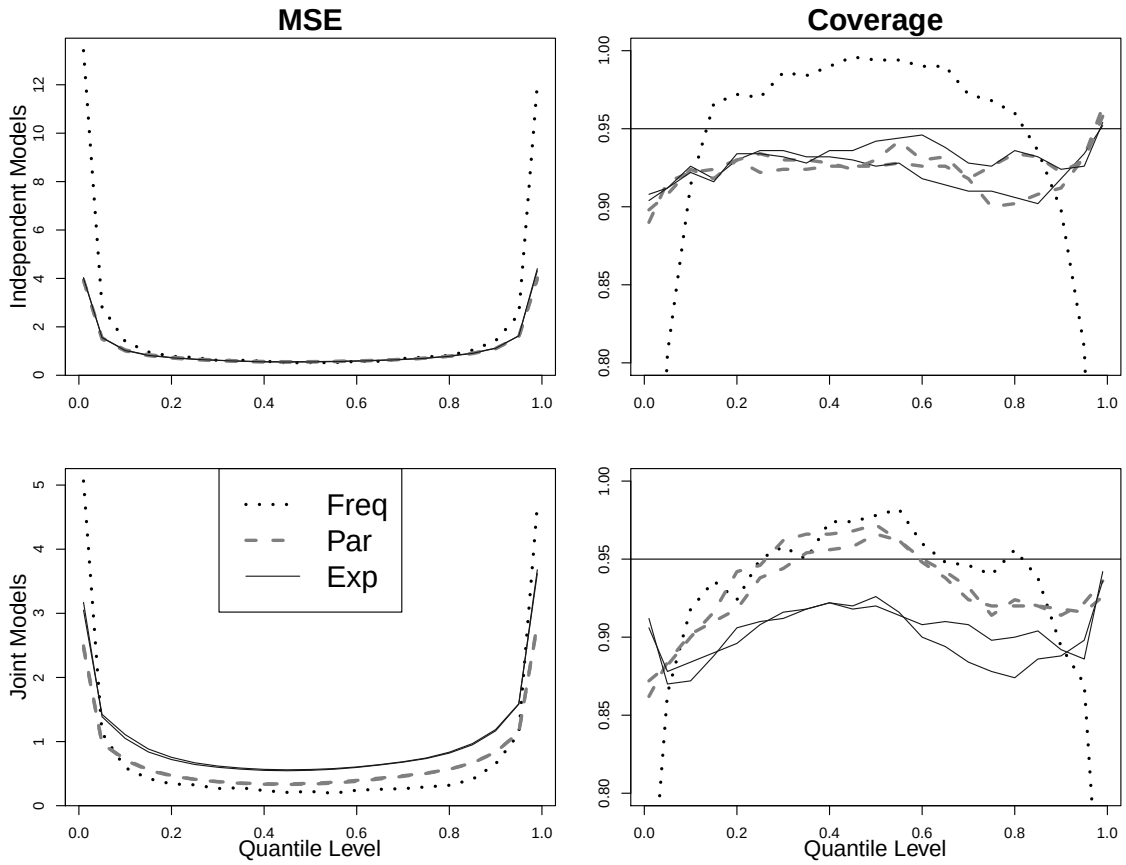

Figure 8. MSE and coverage probabilities for t-distributed response where n = 200 at each gestational age and M = 9. Results above are for the classical frequentist estimator, spline estimator with Pareto tails, and spline estimator with exponential tails, titled "Freq", "Par", and "Exp" respectively.

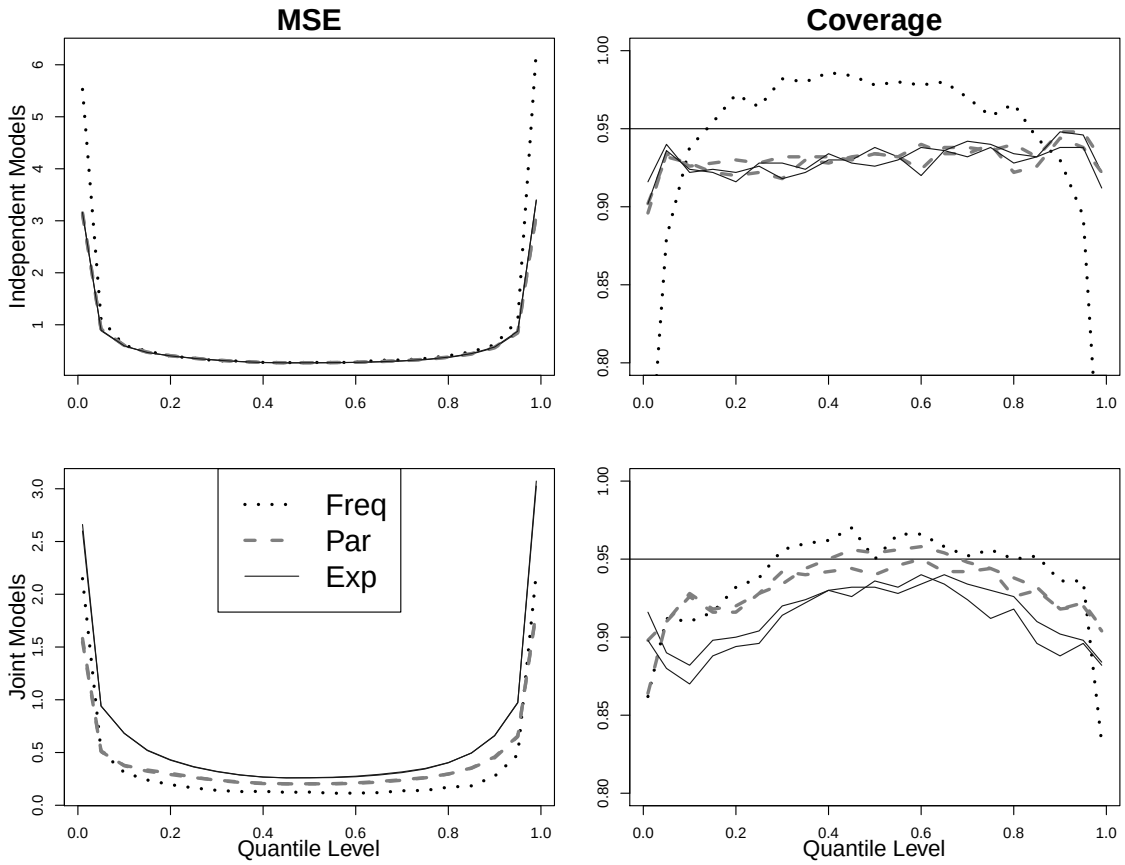

Figure 9. MSE and coverage probabilities for t-distributed response where n = 400 at each gestational age and M = 9. Results above are for the classical frequentist estimator, spline estimator with Pareto tails, and spline estimator with exponential tails, titled "Freq", "Par", and "Exp" respectively.

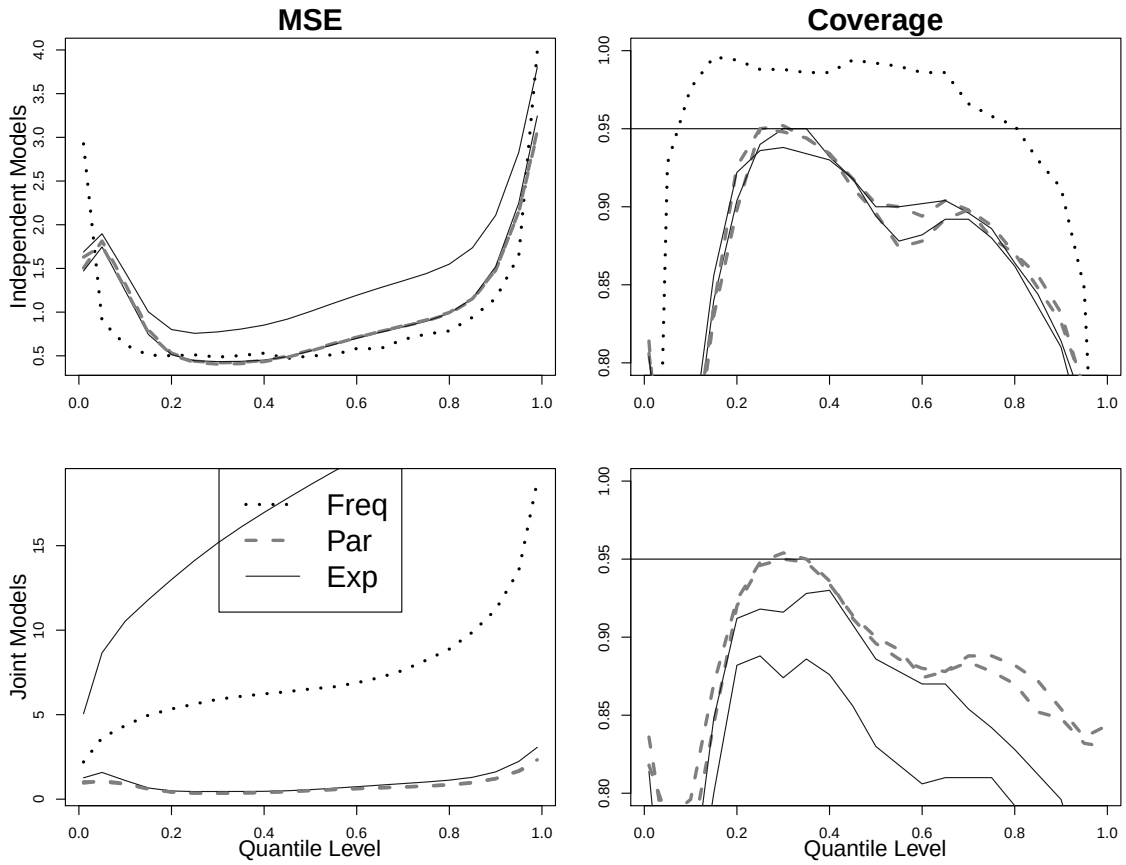

Figure 10. MSE and coverage probabilities for beta-distributed response where n = 200 at each gestational age and M = 5. Results above are for the classical frequentist estimator, spline estimator with Pareto tails, and spline estimator with exponential tails, titled "Freq", "Par", and "Exp" respectively.

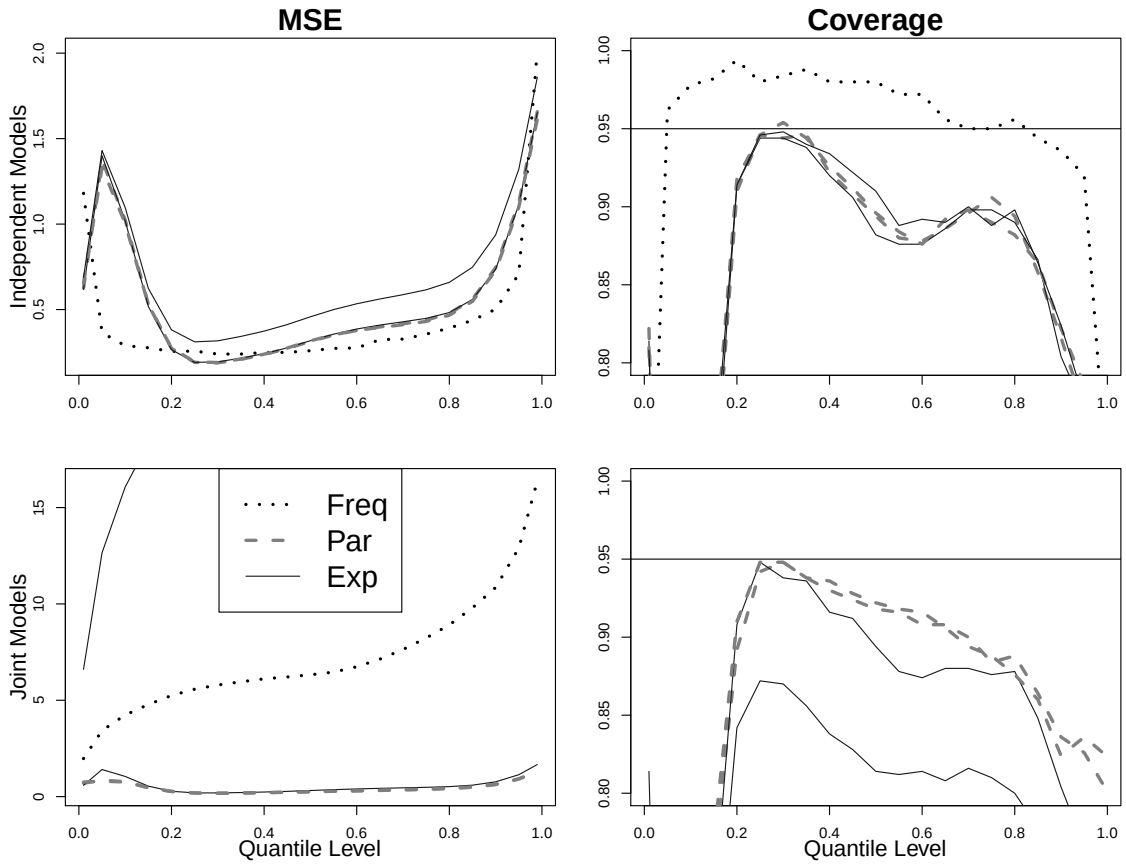

Figure 11. MSE and coverage probabilities for beta-distributed response where n = 400 at each gestational age and M = 5. Results above are for the classical frequentist estimator, spline estimator with Pareto tails, and spline estimator with exponential tails, titled "Freq", "Par", and "Exp" respectively.

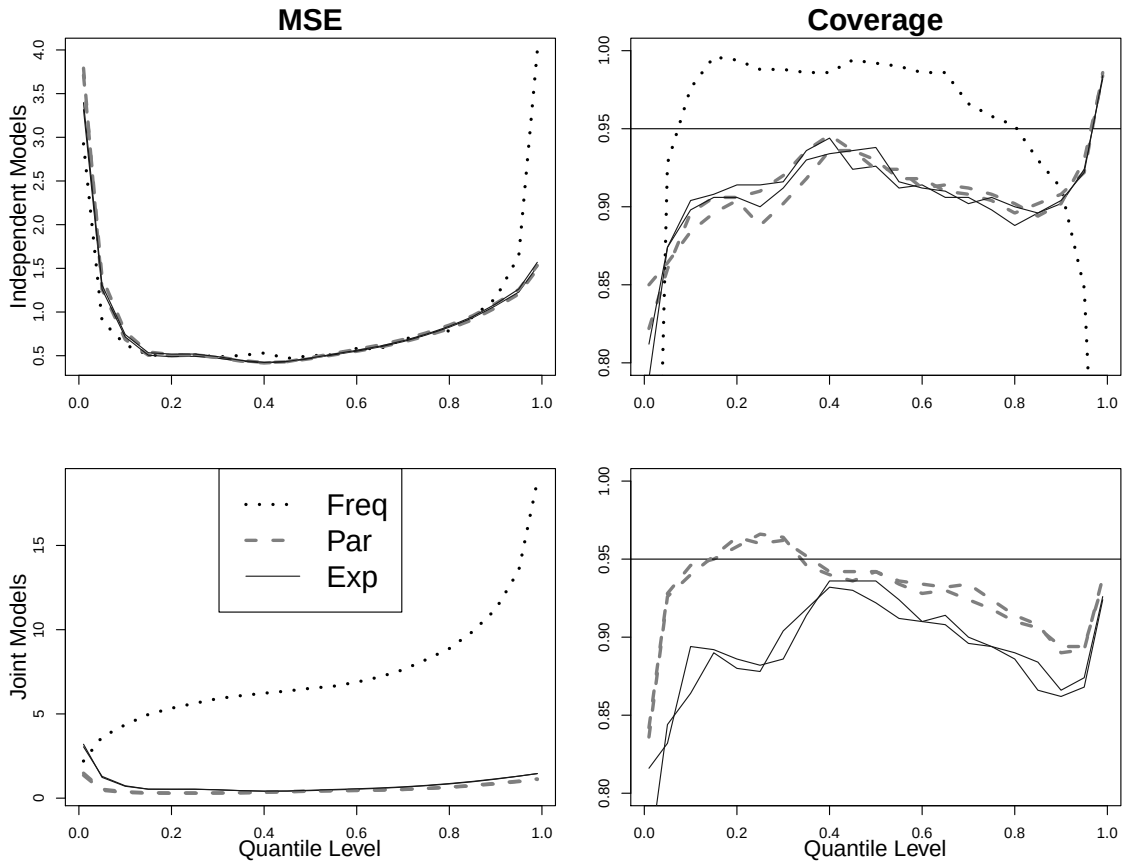

Figure 12. MSE and coverage probabilities for beta-distributed response where n = 200 at each gestational age and M = 7. Results above are for the classical frequentist estimator, spline estimator with Pareto tails, and spline estimator with exponential tails, titled "Freq", "Par", and "Exp" respectively.

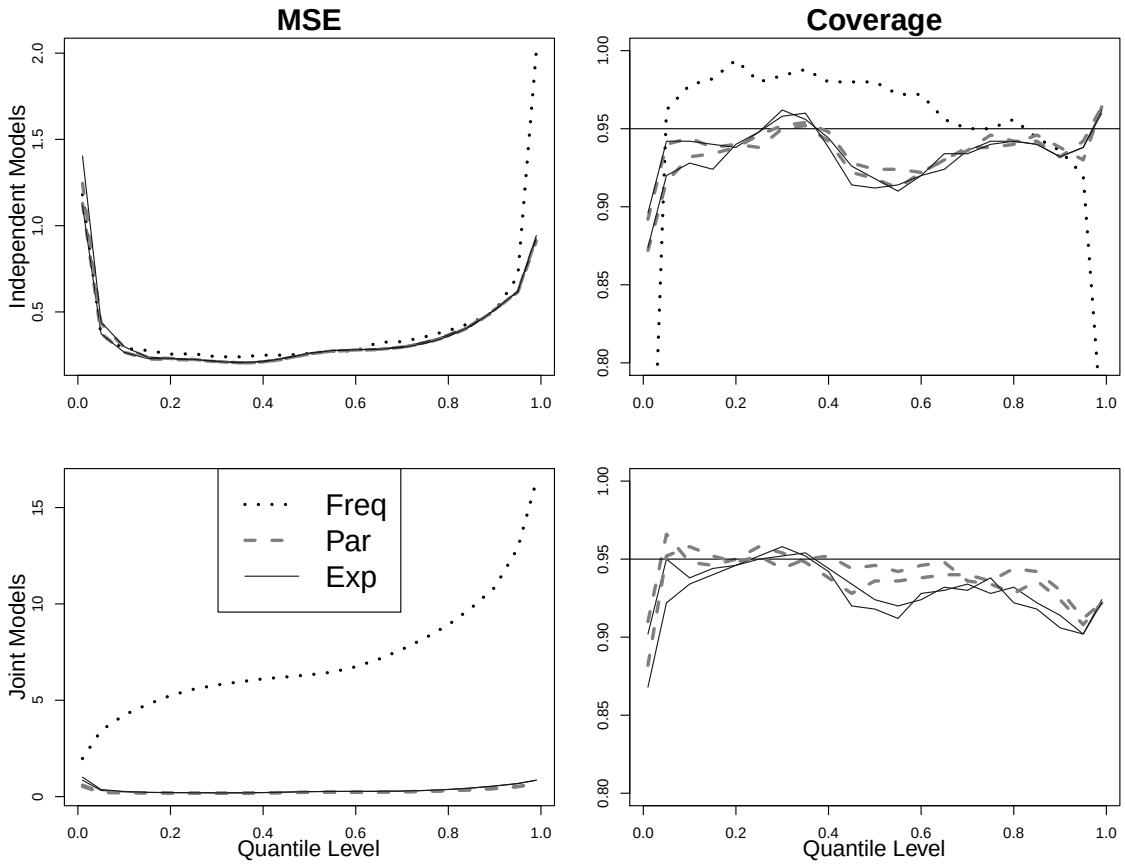

Figure 13. MSE and coverage probabilities for beta-distributed response where n = 400 at each gestational age and M = 7. Results above are for the classical frequentist estimator, spline estimator with Pareto tails, and spline estimator with exponential tails, titled "Freq", "Par", and "Exp" respectively.

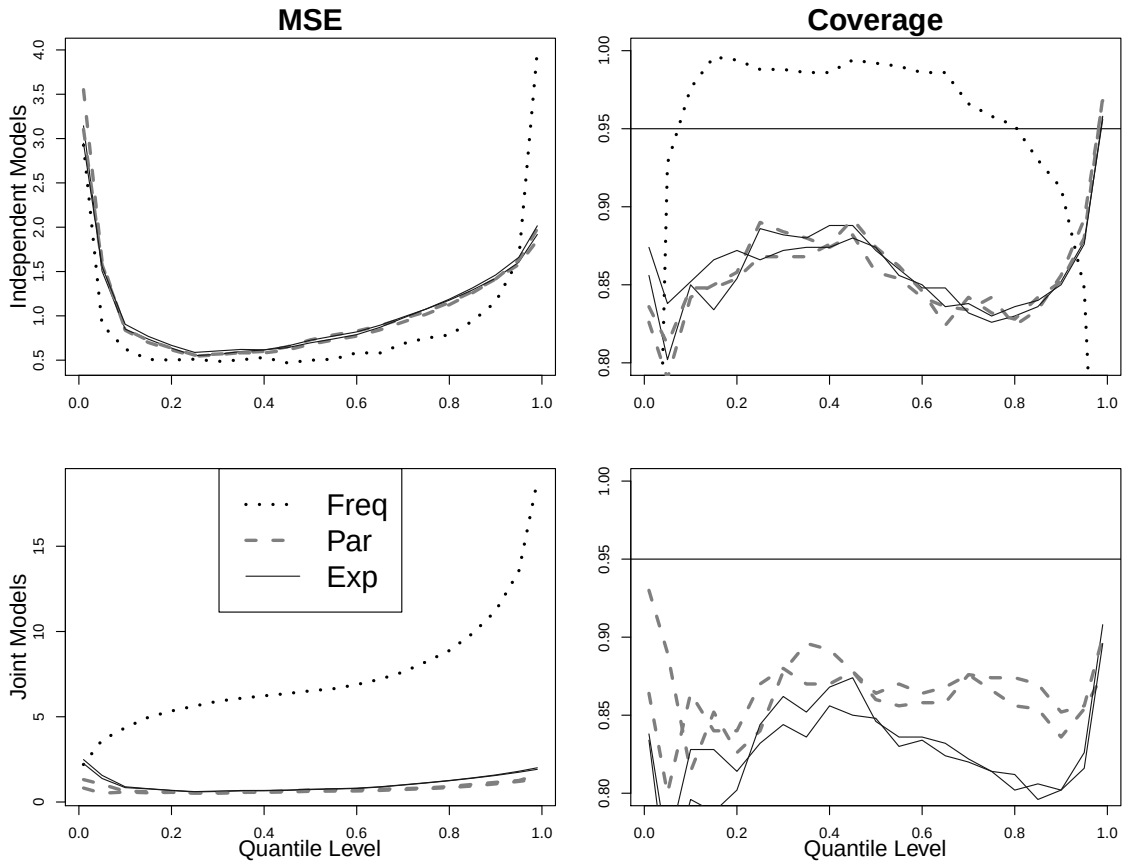

Figure 14. MSE and coverage probabilities for beta-distributed response where n = 200 at each gestational age and M = 9. Results above are for the classical frequentist estimator, spline estimator with Pareto tails, and spline estimator with exponential tails, titled "Freq", "Par", and "Exp" respectively.

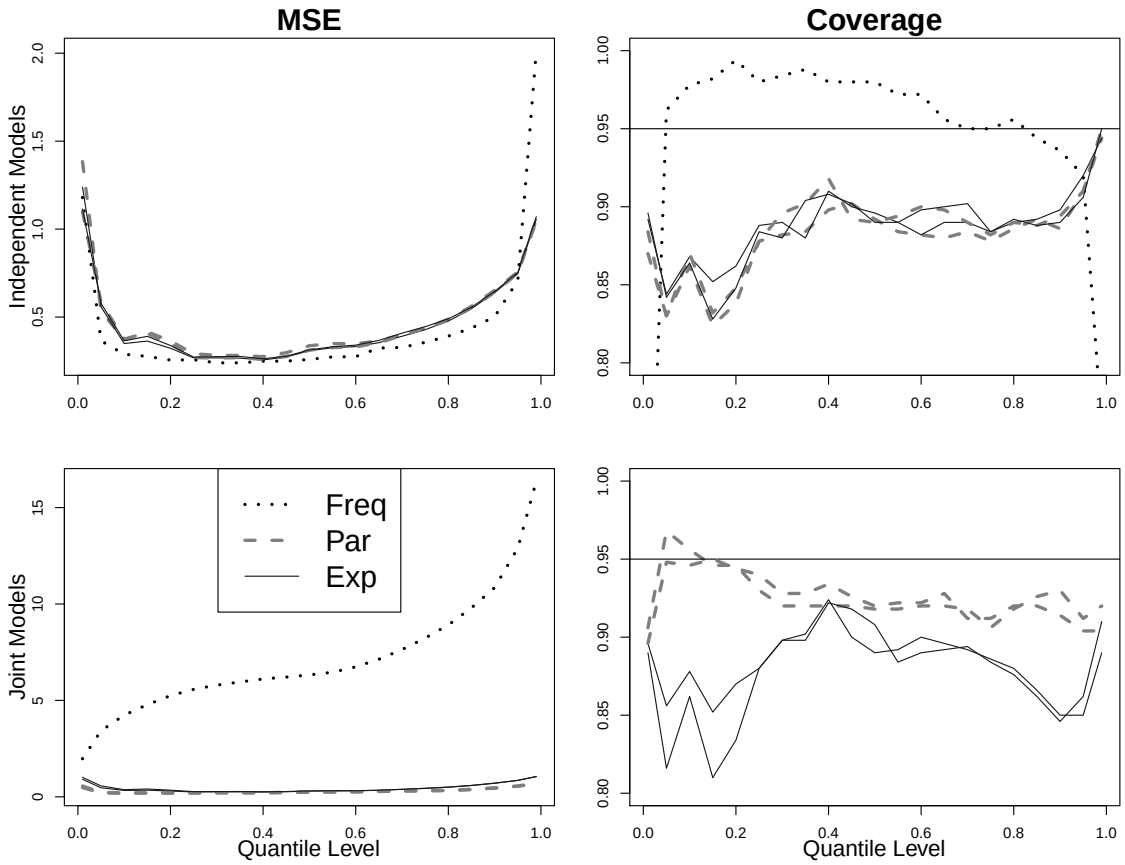

Figure 15. MSE and coverage probabilities for beta-distributed response where n = 400 at each gestational age and M = 9. Results above are for the classical frequentist estimator, spline estimator with Pareto tails, and spline estimator with exponential tails, titled "Freq", "Par", and "Exp" respectively.

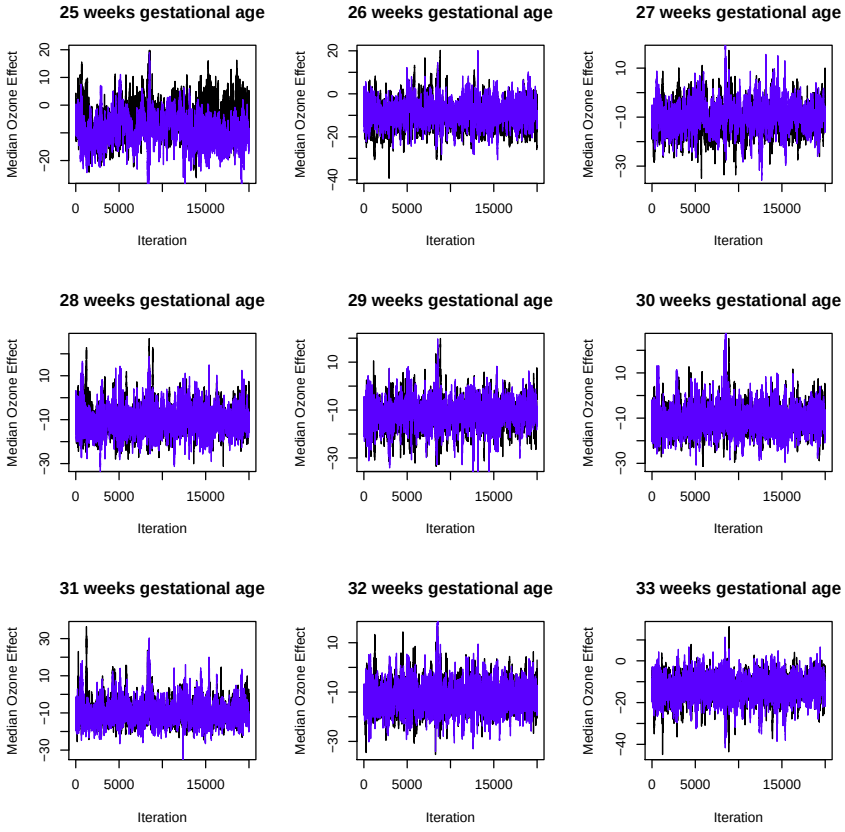

Figure 16. Trace plots of the median regression effect of ozone for two chains with different starting values.

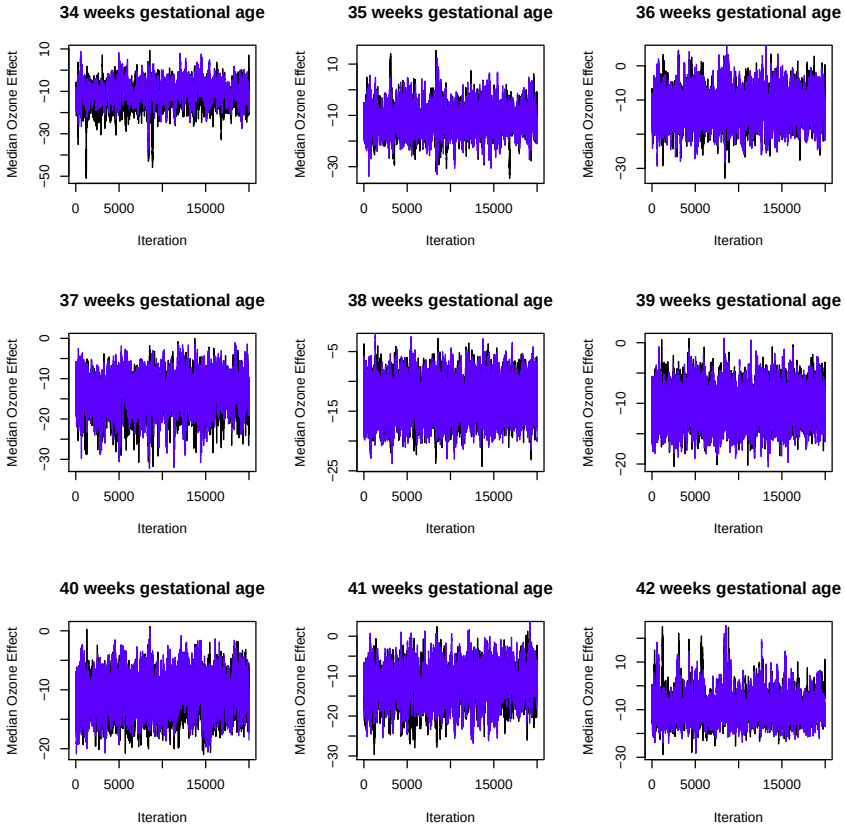

Figure 17. Trace plots of the median regression effect of ozone for two chains with different starting values.

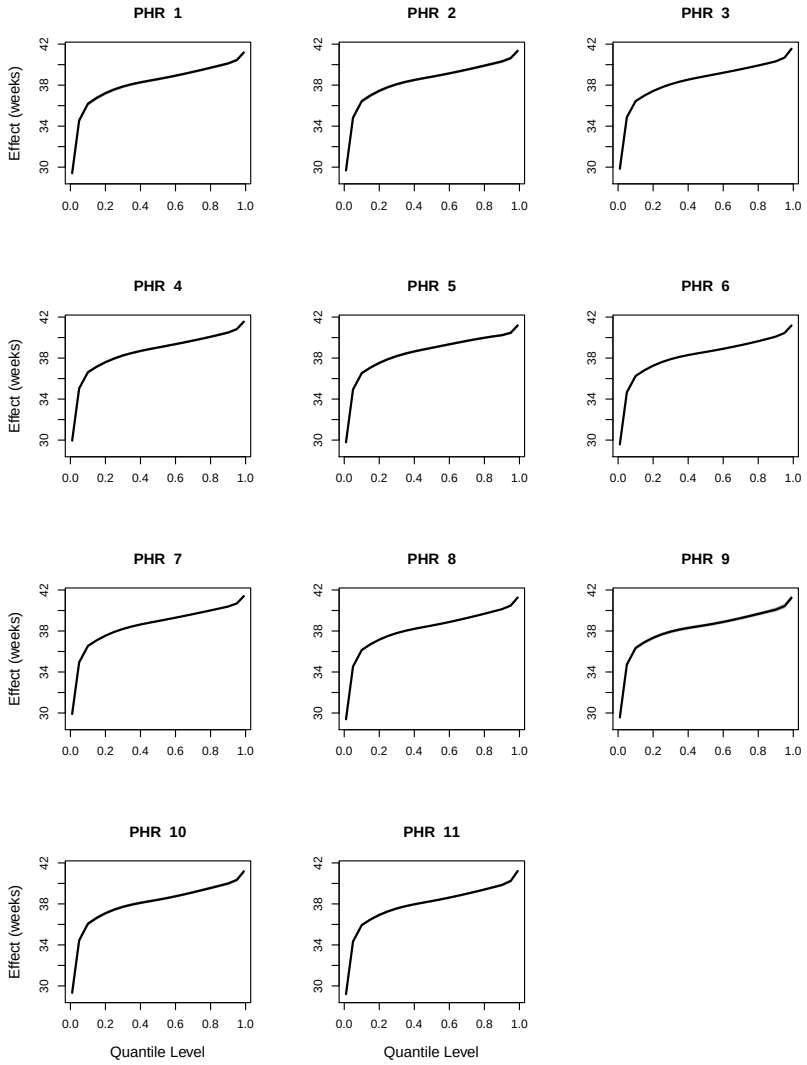

Figure 18. 95% credible limits for the posterior distribution of the intercept process for gestational age by Public Health Region (PHR). The intercept process represents the information regarding gestational age not explained by the predictors and was permitted to vary by PHR. The intercept process is not interpretable, as we had binary variables that were valued at either -1 or 1.

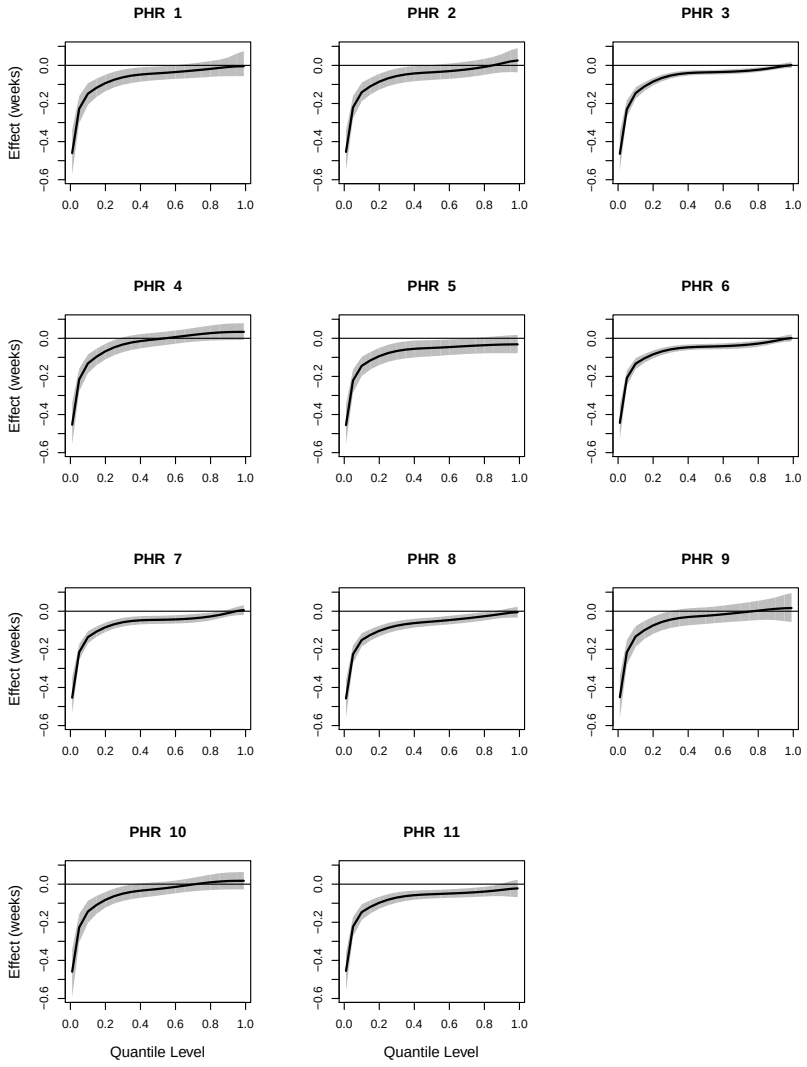

Figure 19. 95% credible limits for the posterior distribution of the effect of being male vs. female on gestational age by Public Health Region (PHR).

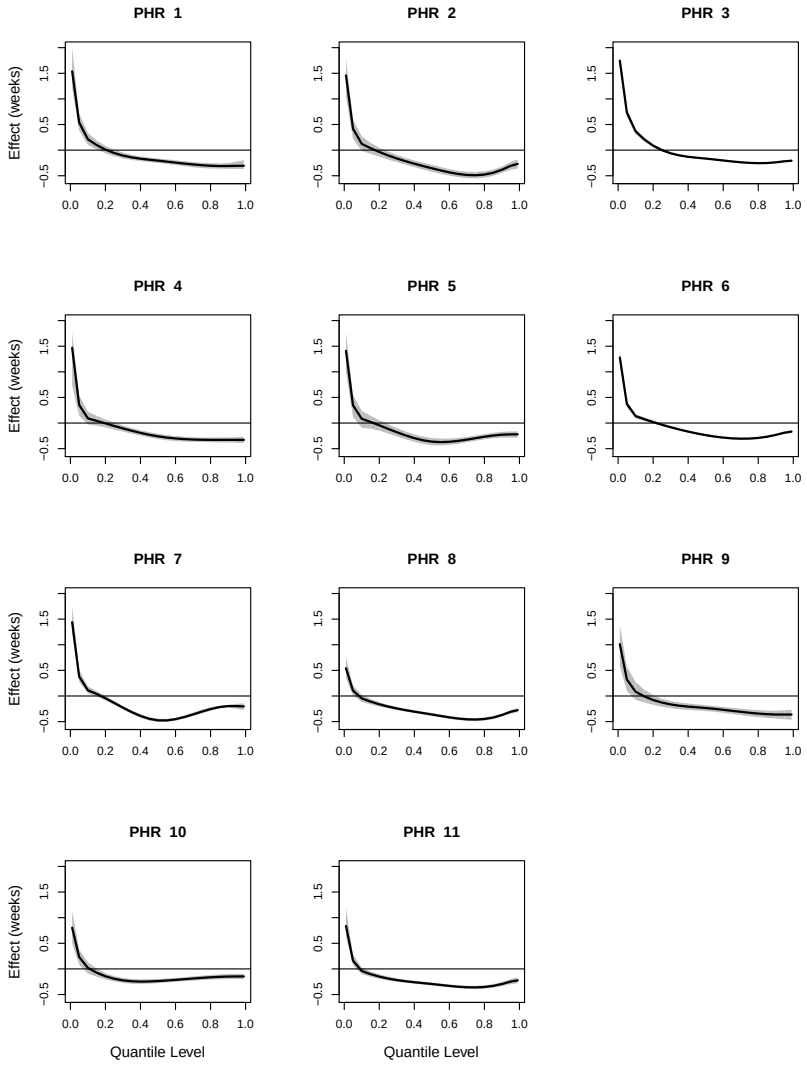

Figure 20. 95% credible limits for the posterior distribution of the effect of maternal parity on gestational age by Public Health Region (PHR).

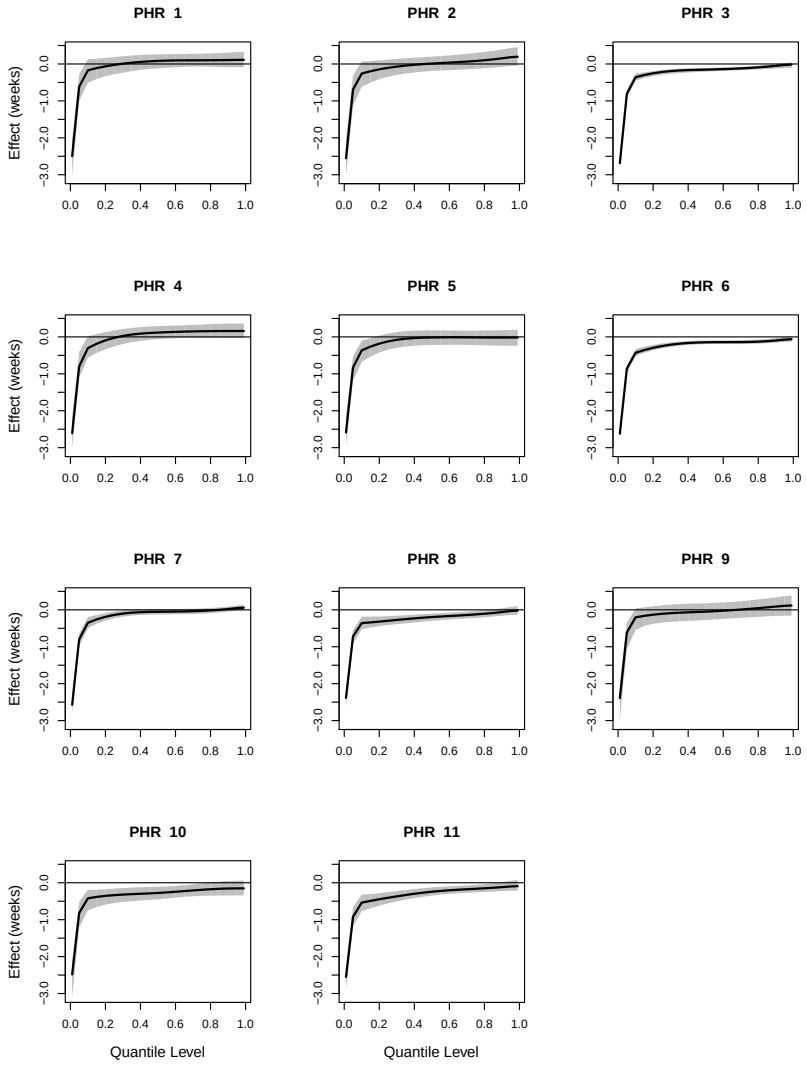

Figure 21. 95% credible limits for the posterior distribution of the effect of maternal age 40 and above on gestational age by Public Health Region (PHR).

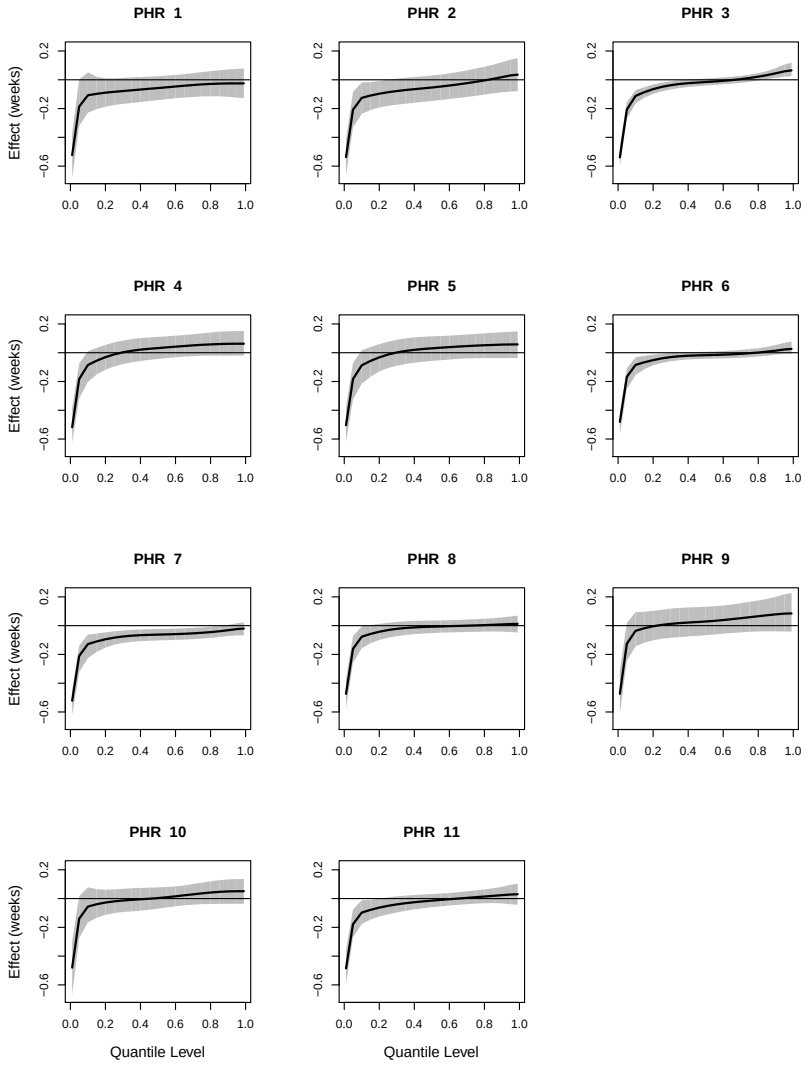

Figure 22. 95% credible limits for the posterior distribution of the effect of paternal age 40 and above on gestational age by Public Health Region (PHR).

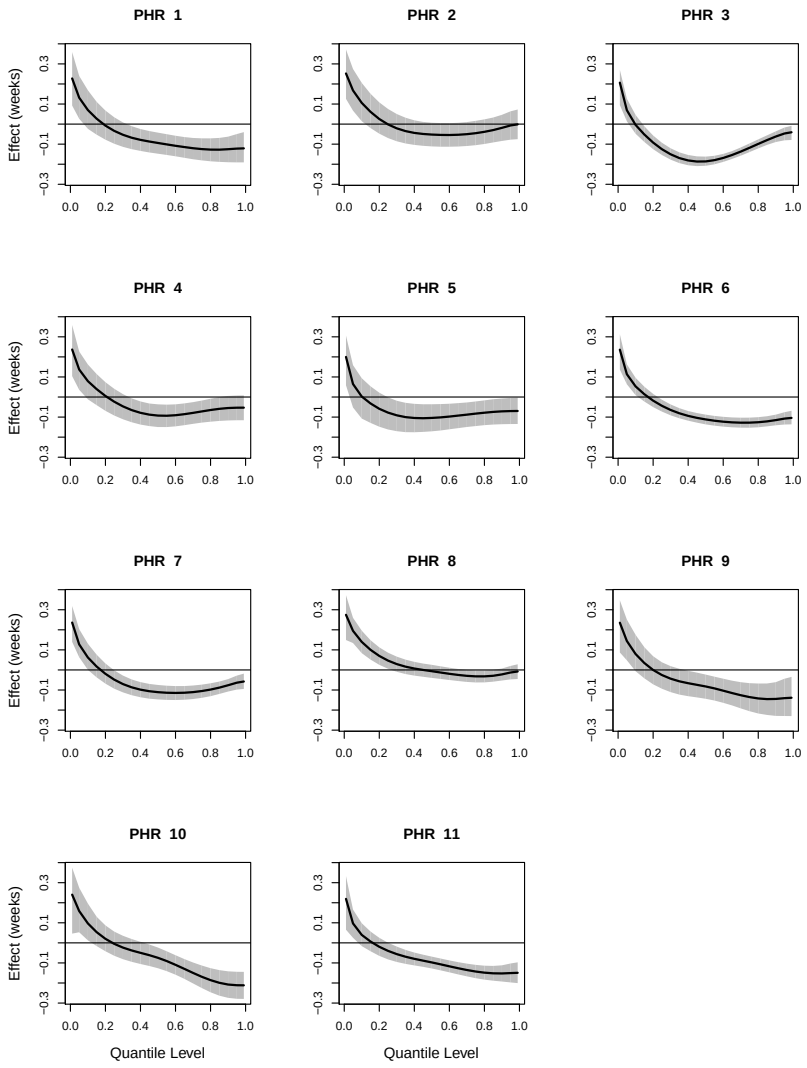

Figure 23. 95% credible limits for the posterior distribution of the effect of the mother finishing high school relative to not finishing high school on gestational age by Public Health Region (PHR).

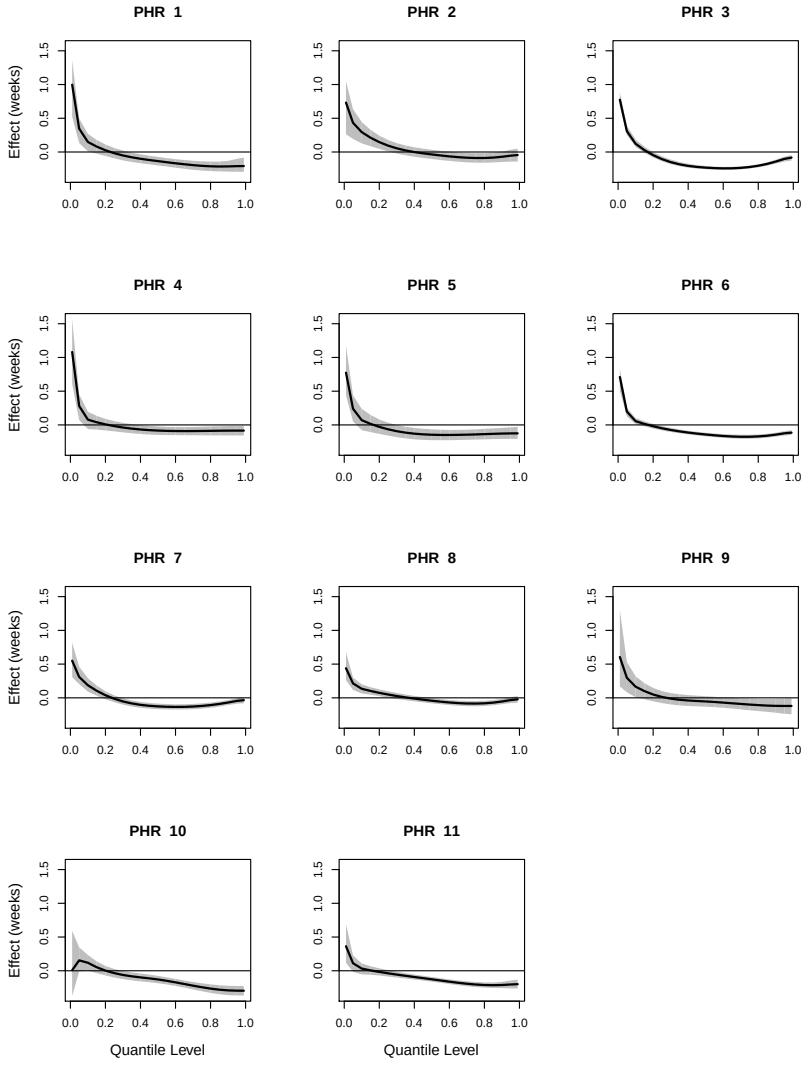

Figure 24. 95% credible limits for the posterior distribution of the effect of the mother finishing education above high school relative to not finishing high school on gestational age by Public Health Region (PHR).

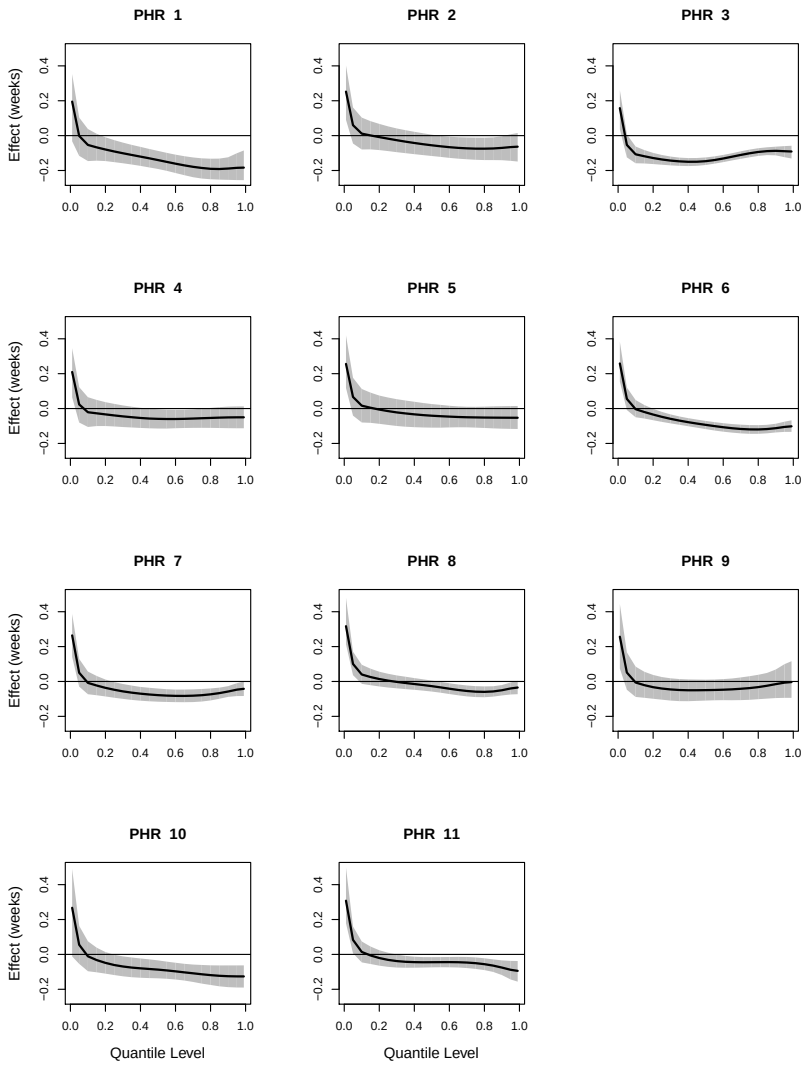

Figure 25. 95% credible limits for the posterior distribution of the effect of the father finishing high school relative to not finishing high school on gestational age by Public Health Region (PHR).

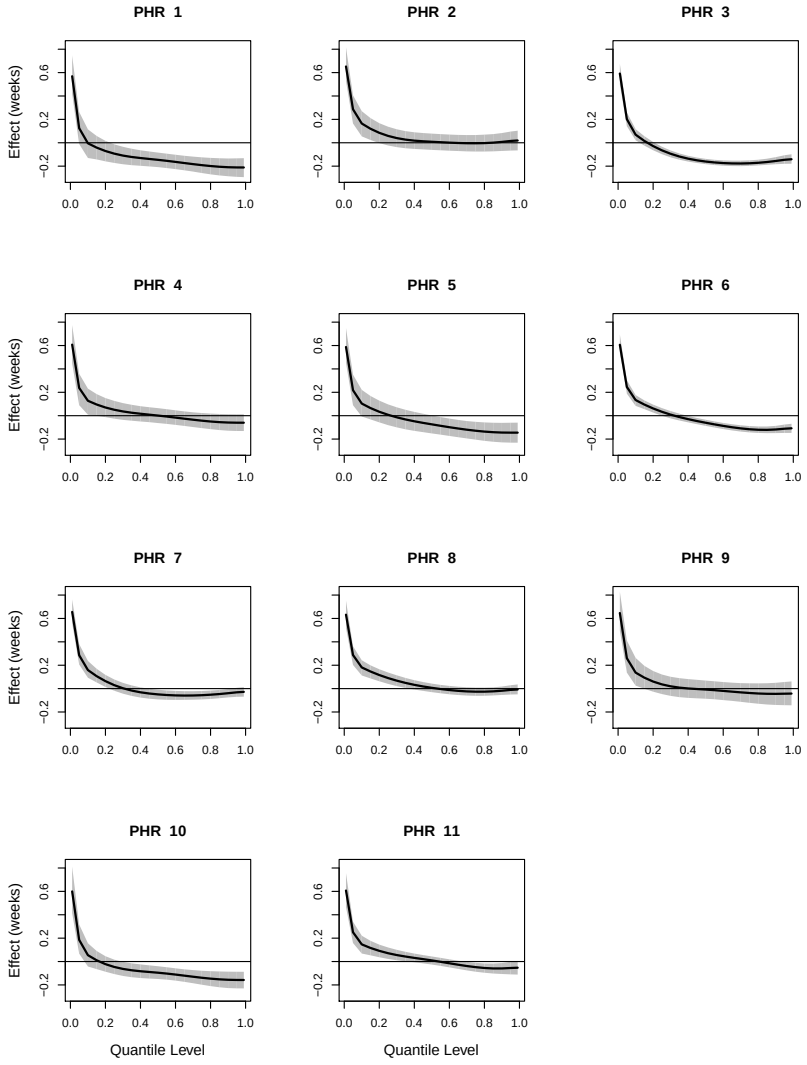

Figure 26. 95% credible limits for the posterior distribution of the effect of the father finishing education above high school relative to not finishing high school on gestational age by Public Health Region (PHR).

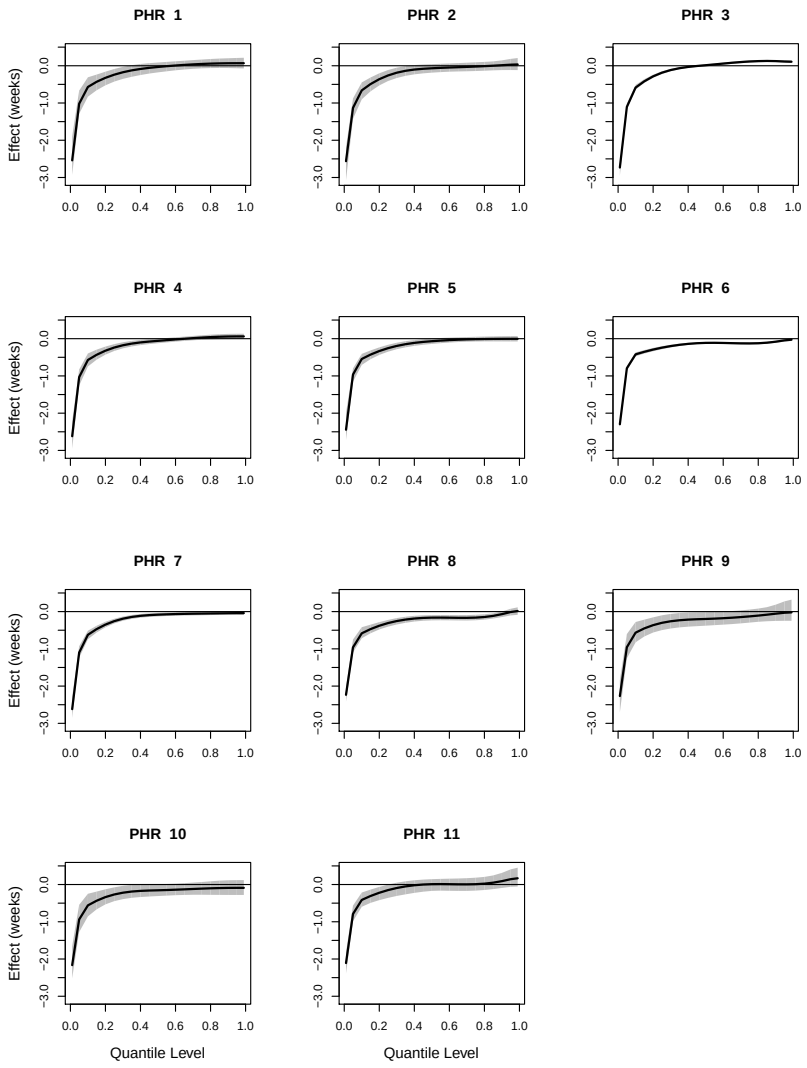

Figure 27. 95% credible limits for the posterior distribution of the effect of black non-Hispanic maternal ethnicity relative to white non-Hispanic maternal ethnicity on gestational age by Public Health Region (PHR).

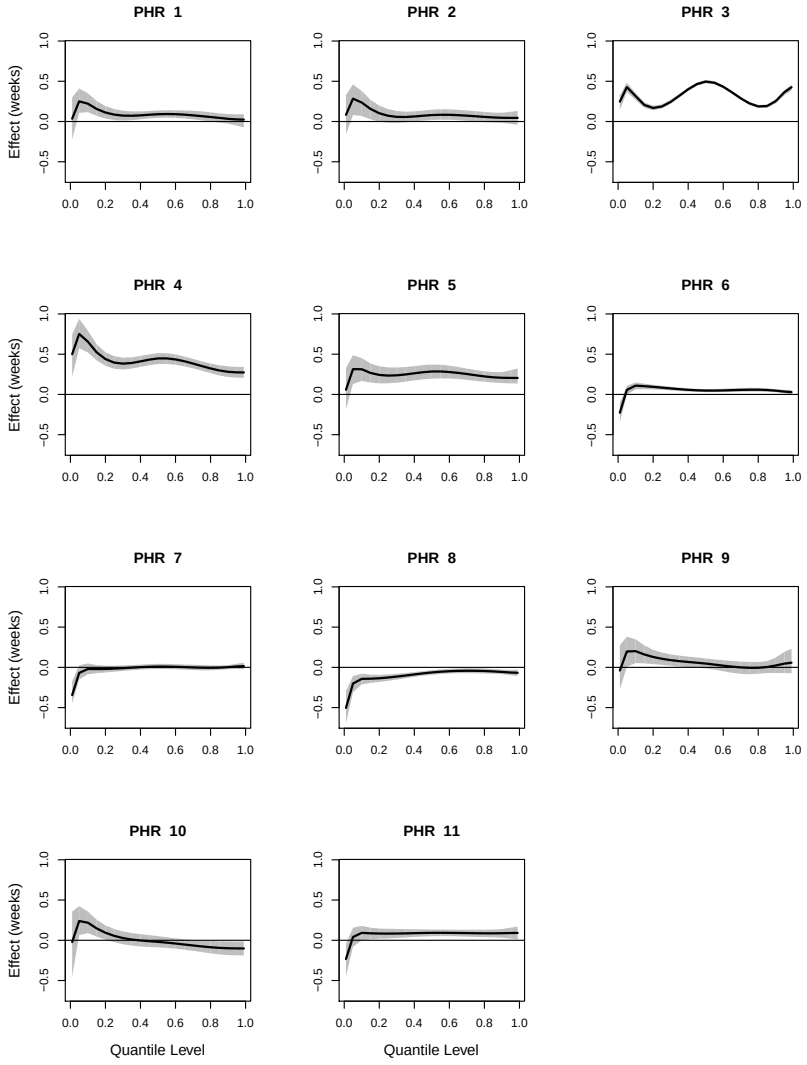

Figure 28. 95% credible limits for the posterior distribution of the effect of Hispanic maternal ethnicity relative to white non-Hispanic maternal ethnicity on gestational age by Public Health Region (PHR).

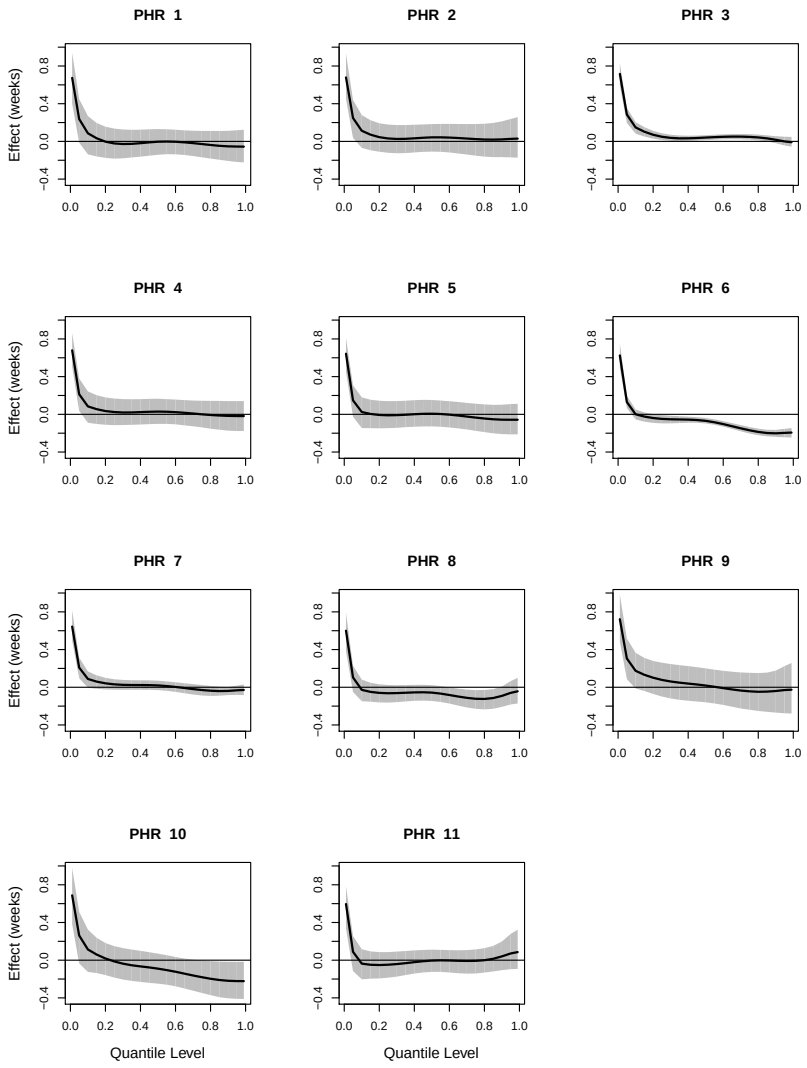

Figure 29. 95% credible limits for the posterior distribution of the effect of other maternal ethnicity relative to white non-Hispanic maternal ethnicity on gestational age by Public Health Region (PHR).

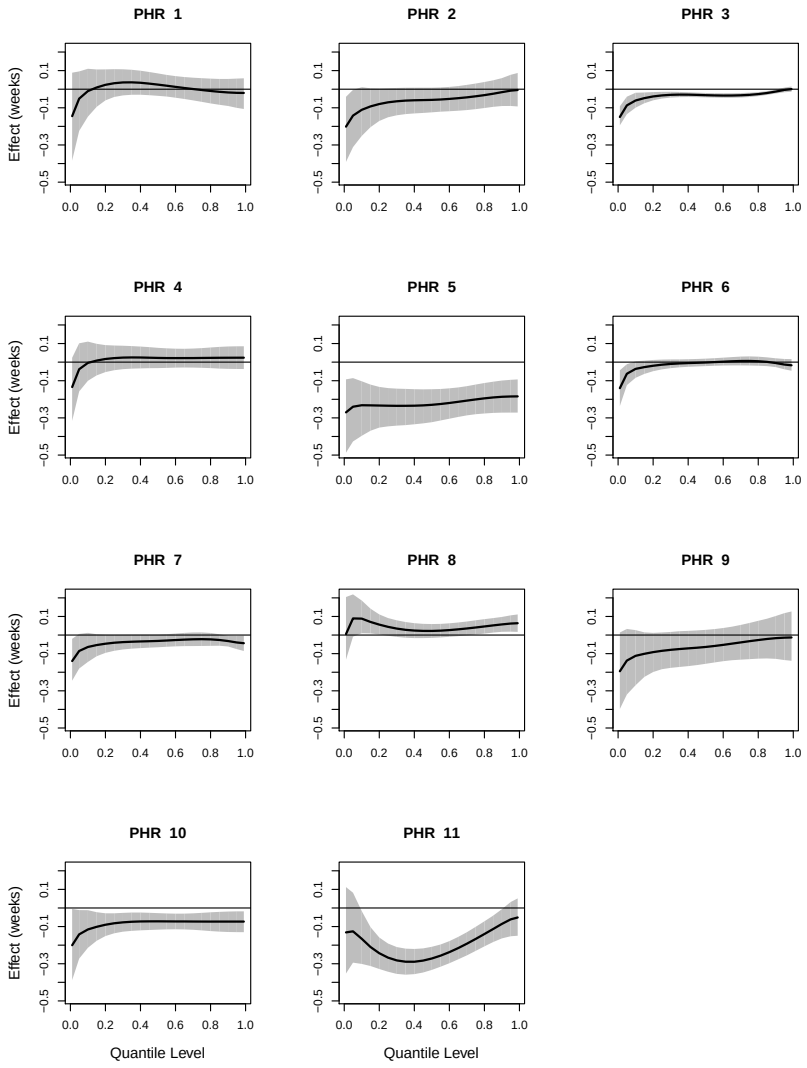

Figure 30. 95% credible limits for the posterior distribution of the effect of a one-unit increase in first trimester ozone exposure on gestational age by Public Health Region (PHR). All ozone values were linearly transformed into [-1,1], so a one-unit increase can be roughly thought of as an increase from low levels to middle levels of exposure, or middle to high.

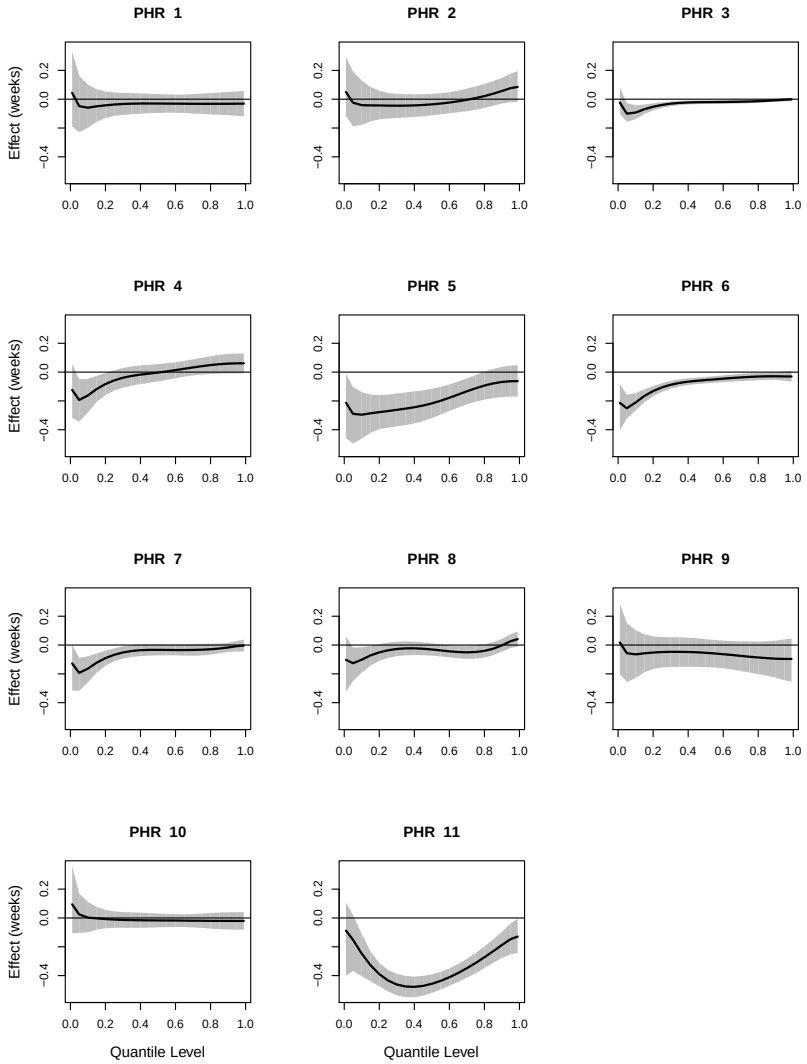

Figure 31. 95% credible limits for the posterior distribution of the effect of a one-unit increase in second trimester ozone exposure on gestational age by Public Health Region (PHR). All ozone values were linearly transformed into [-1,1], so a one-unit increase can be roughly thought of as an increase from low levels to middle levels of exposure, or middle to high.

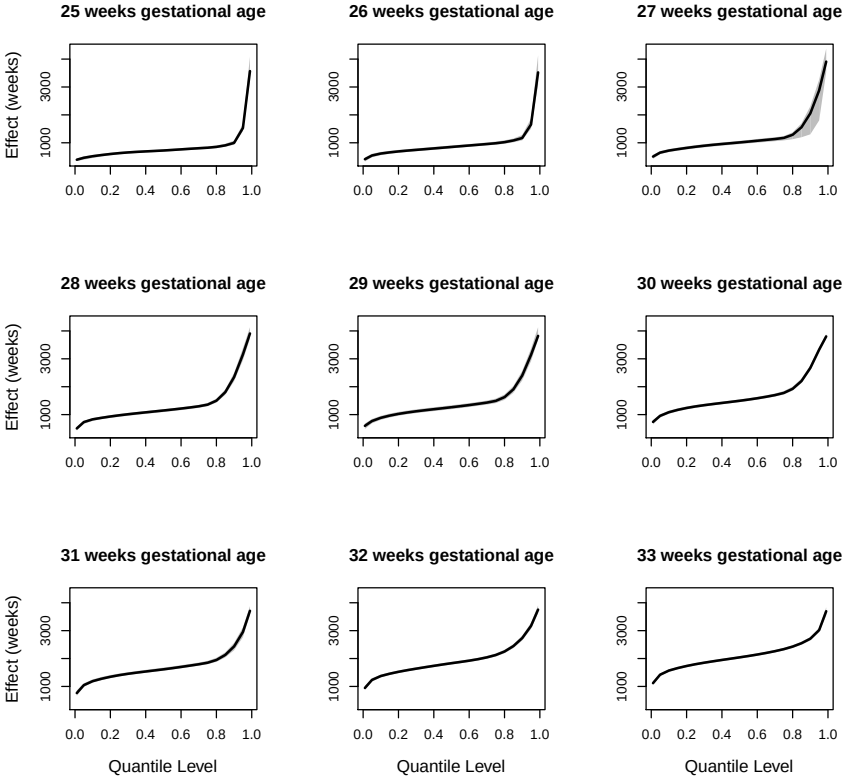

Figure 32. 95% credible limits for the posterior distribution of the intercept of birth weight for gestational ages 25-33 weeks.

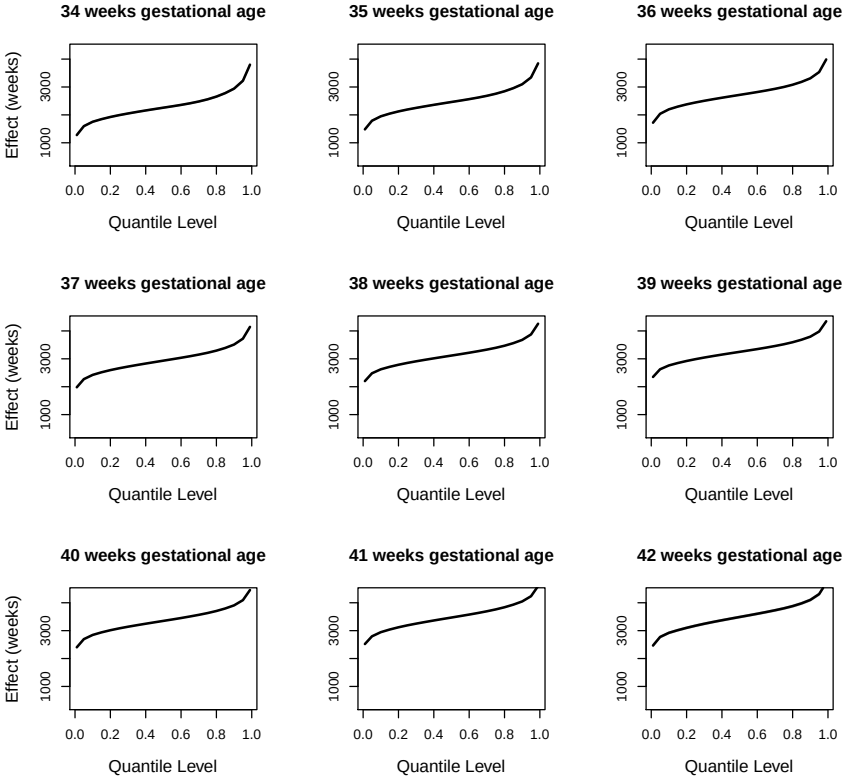

Figure 33. 95% credible limits for the posterior distribution of the intercept of birth weight for gestational ages 34-42 weeks.

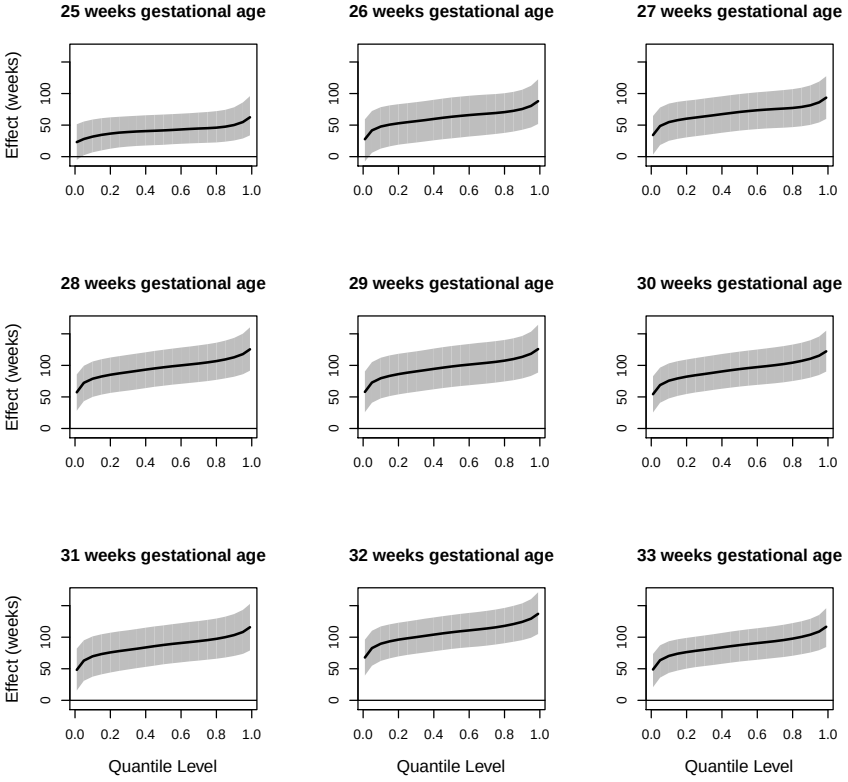

Figure 34. 95% credible limits for the posterior distribution of the effect of male sex relative to female on birth weight for gestational ages 25-33 weeks.

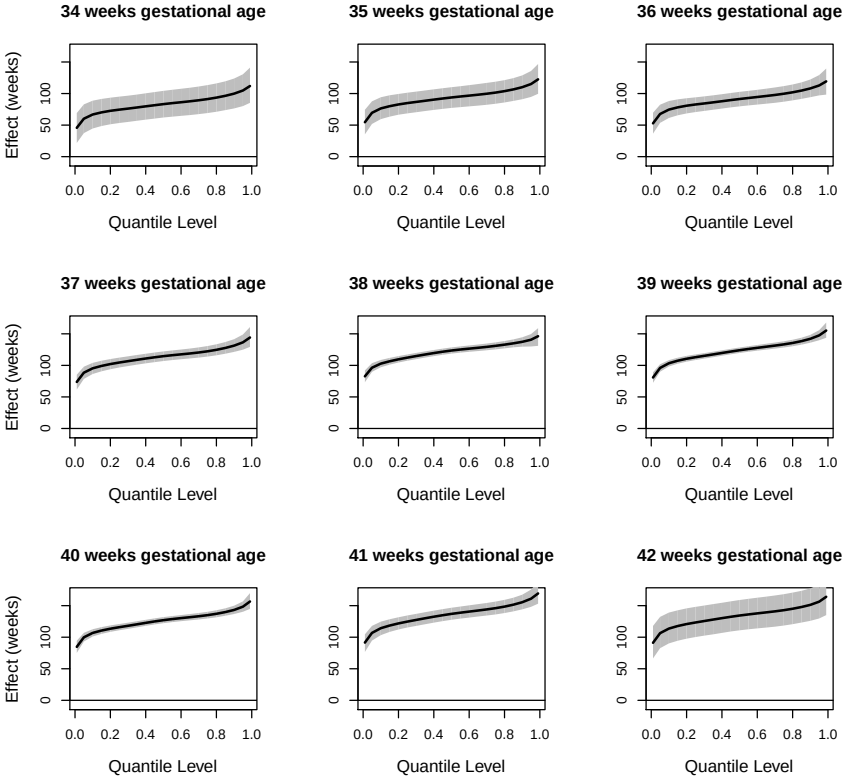

Figure 35. 95% credible limits for the posterior distribution of the effect of male sex relative to female on birth weight for gestational ages 34-42 weeks.

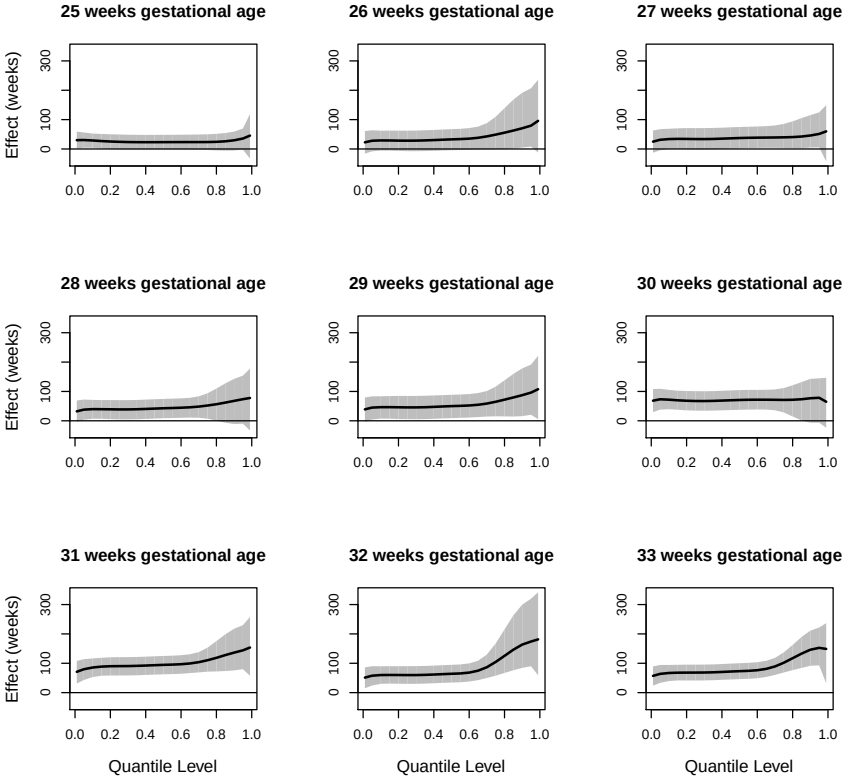

Figure 36. 95% credible limits for the posterior distribution of the effect of maternal parity on birth weight for gestational ages 25-33 weeks.

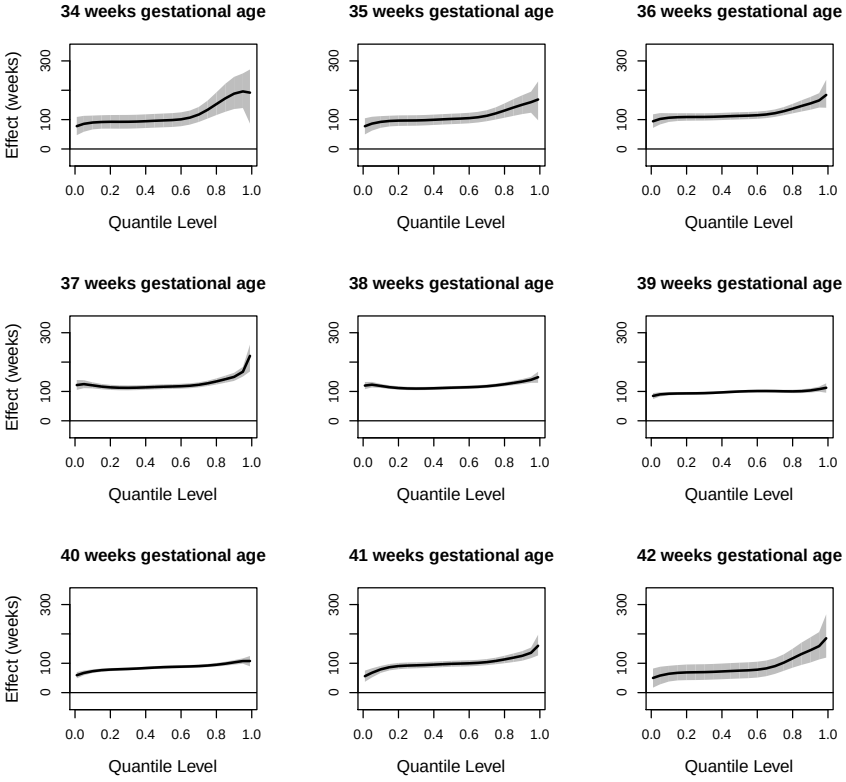

Figure 37. 95% credible limits for the posterior distribution of the effect of maternal parity on birth weight for gestational ages 34-42 weeks.

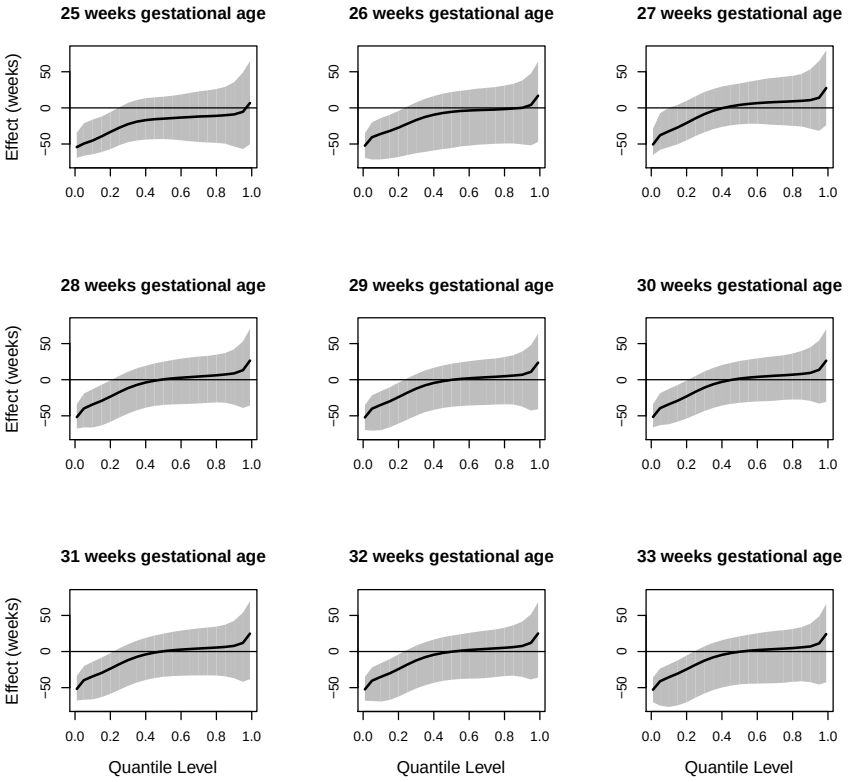

Figure 38. 95% credible limits for the posterior distribution of the effect of maternal age greater than 40 relative to maternal age less than 40 on birth weight for gestational ages 25-33 weeks.

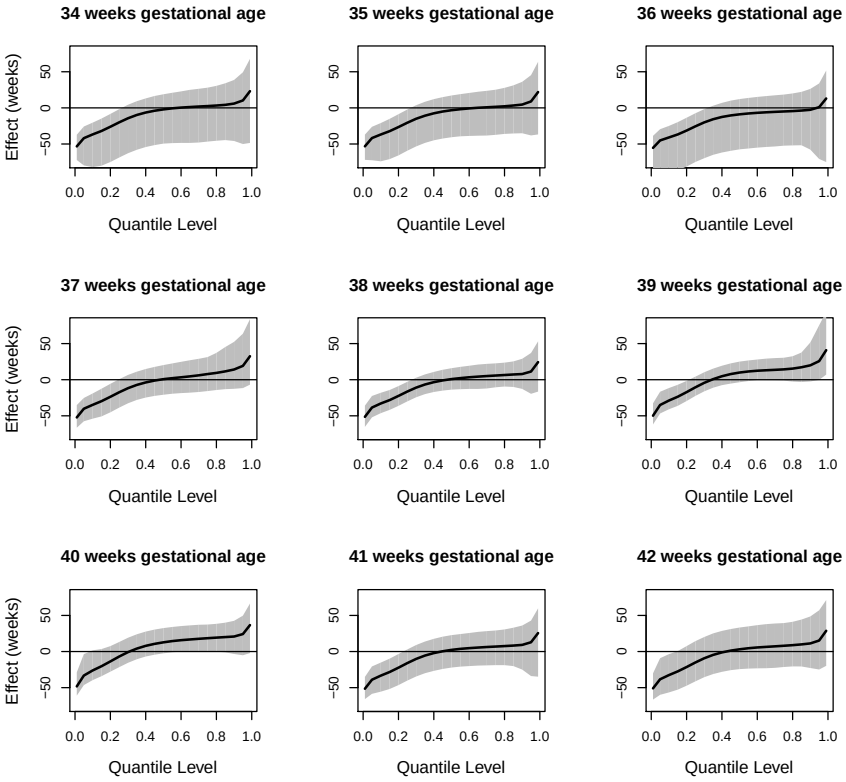

Figure 39. 95% credible limits for the posterior distribution of the effect of maternal age greater than 40 relative to maternal age less than 40 on birth weight for gestational ages 34-42 weeks.

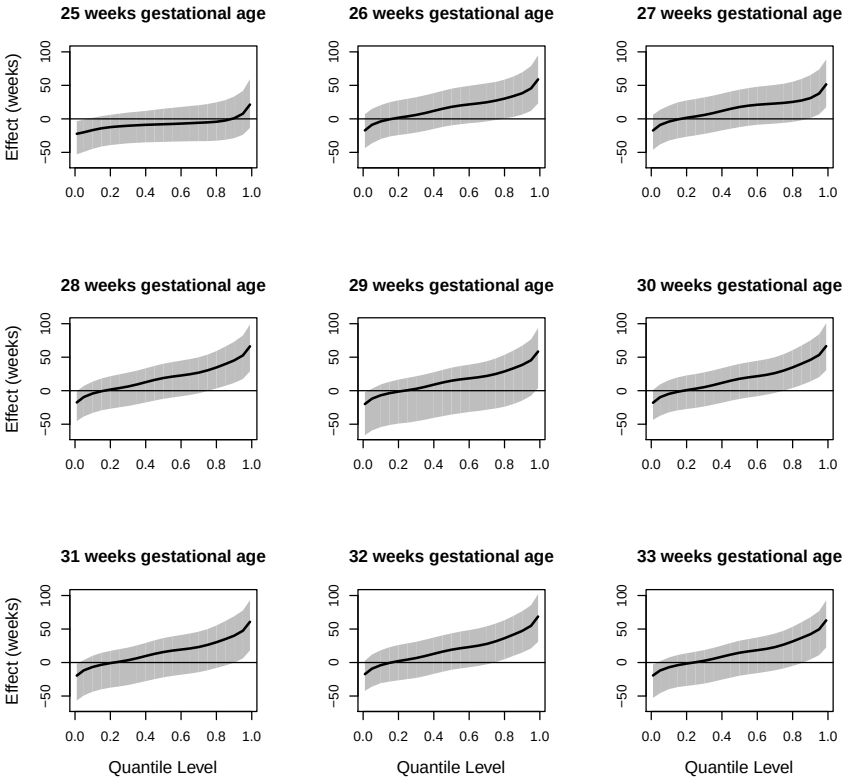

Figure 40. 95% credible limits for the posterior distribution of the effect of paternal age greater than 40 relative to paternal age less than 40 on birth weight for gestational ages 25-33 weeks.

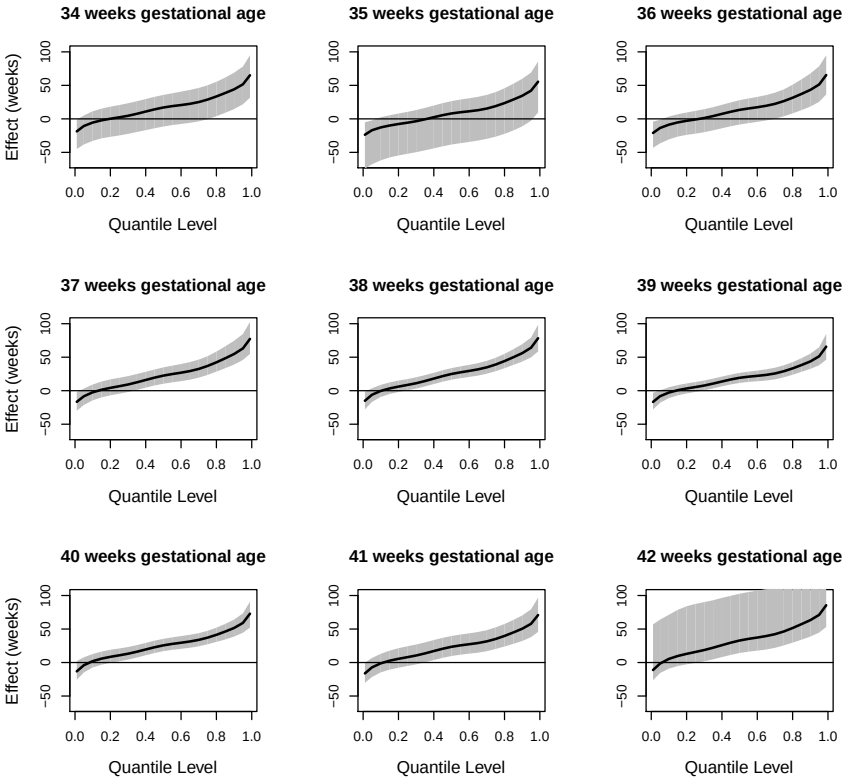

Figure 41. 95% credible limits for the posterior distribution of the effect of paternal age greater than 40 relative to paternal age less than 40 on birth weight for gestational ages 34-42 weeks.

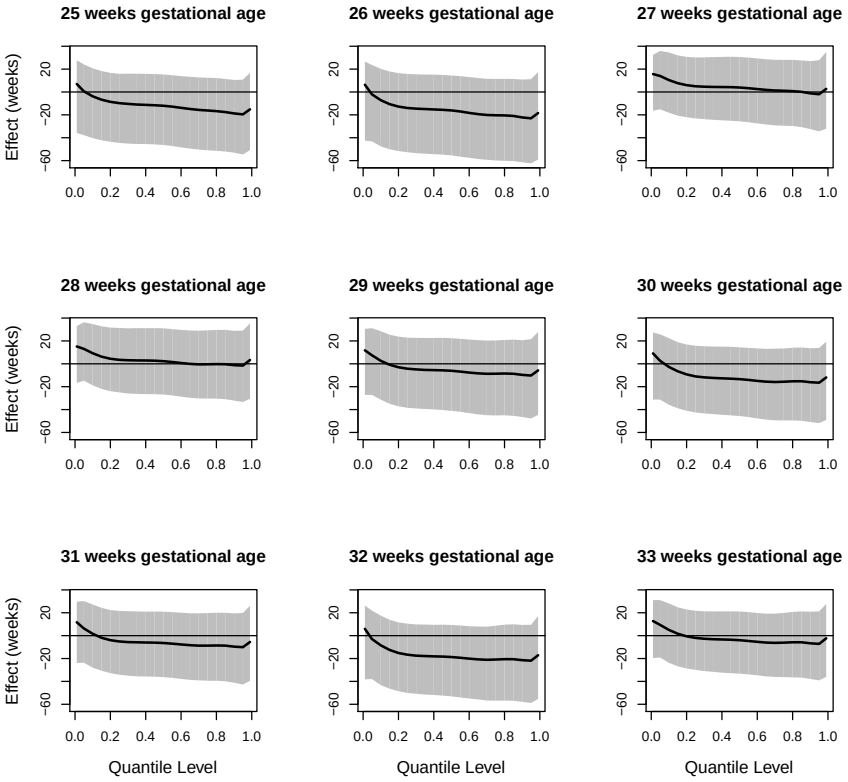

Figure 42. 95% credible limits for the posterior distribution of the effect of the mother finishing high school relative to not finishing high school on birth weight for gestational ages 25-33 weeks.

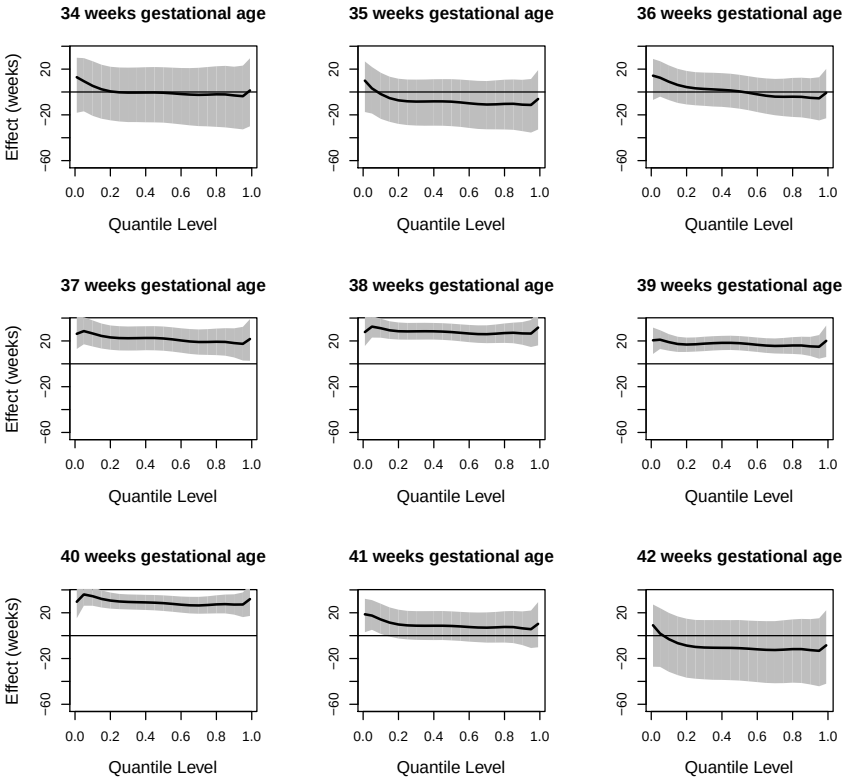

Figure 43. 95% credible limits for the posterior distribution of the effect of the mother finishing high school relative to not finishing high school on birth weight for gestational ages 34-42 weeks.

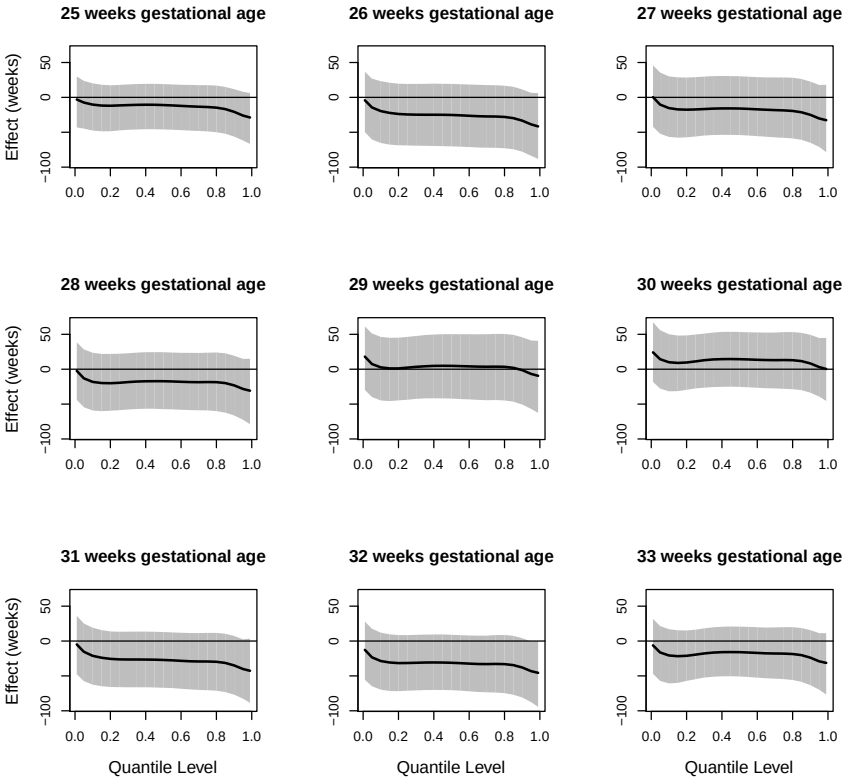

Figure 44. 95% credible limits for the posterior distribution of the effect of the mother finishing education above high school relative to not finishing high school on birth weight for gestational ages 25-33 weeks.

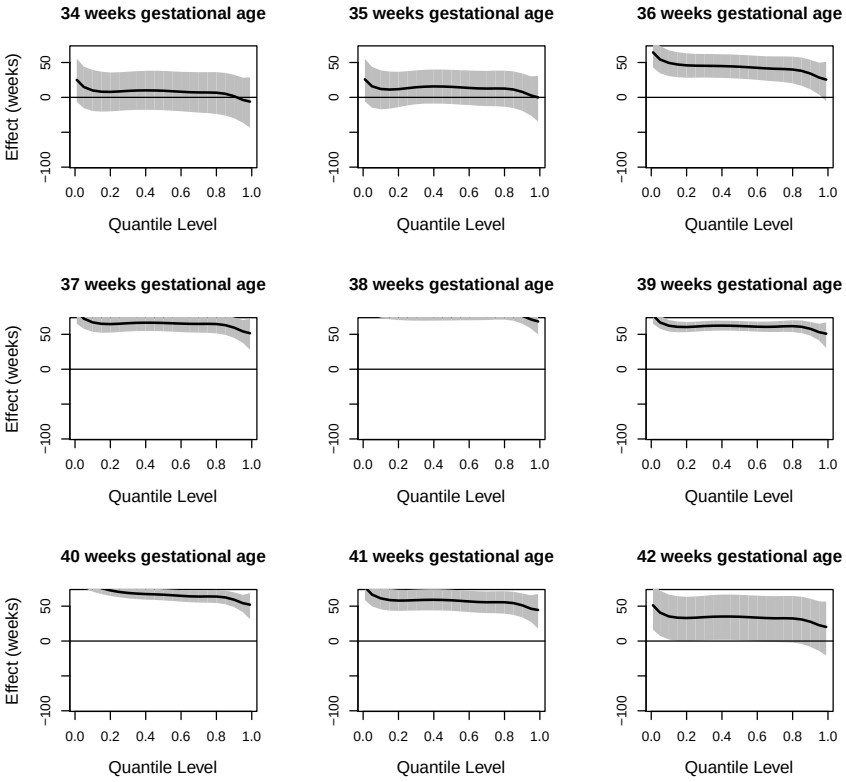

Figure 45. 95% credible limits for the posterior distribution of the effect of the mother finishing education above high school relative to not finishing high school on birth weight for gestational ages 34-42 weeks.

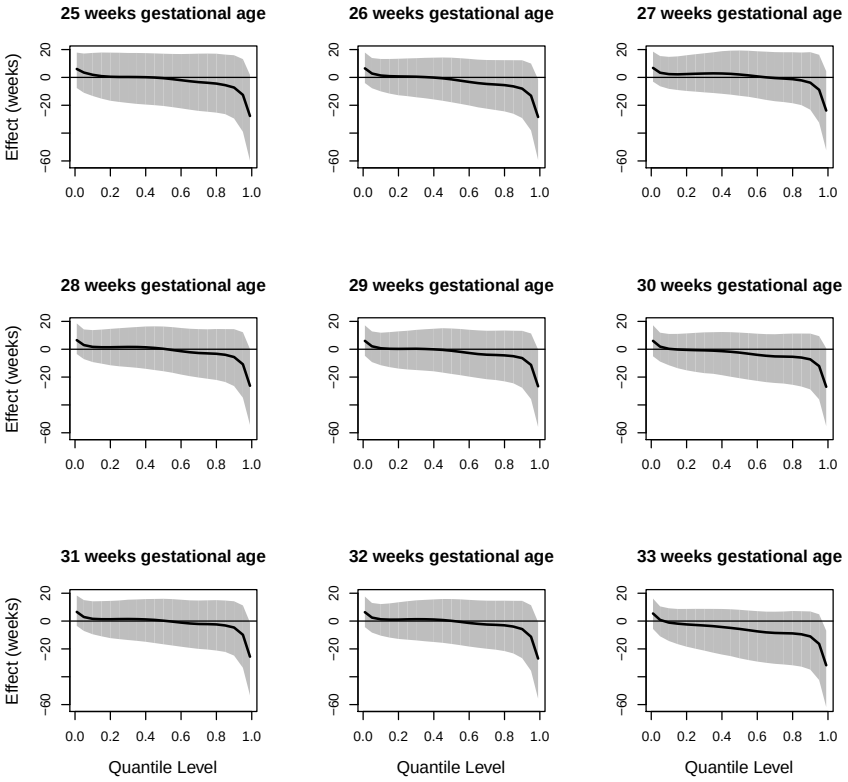

Figure 46. 95% credible limits for the posterior distribution of the effect of the father finishing high school relative to not finishing high school on birth weight for gestational ages 25-33 weeks.

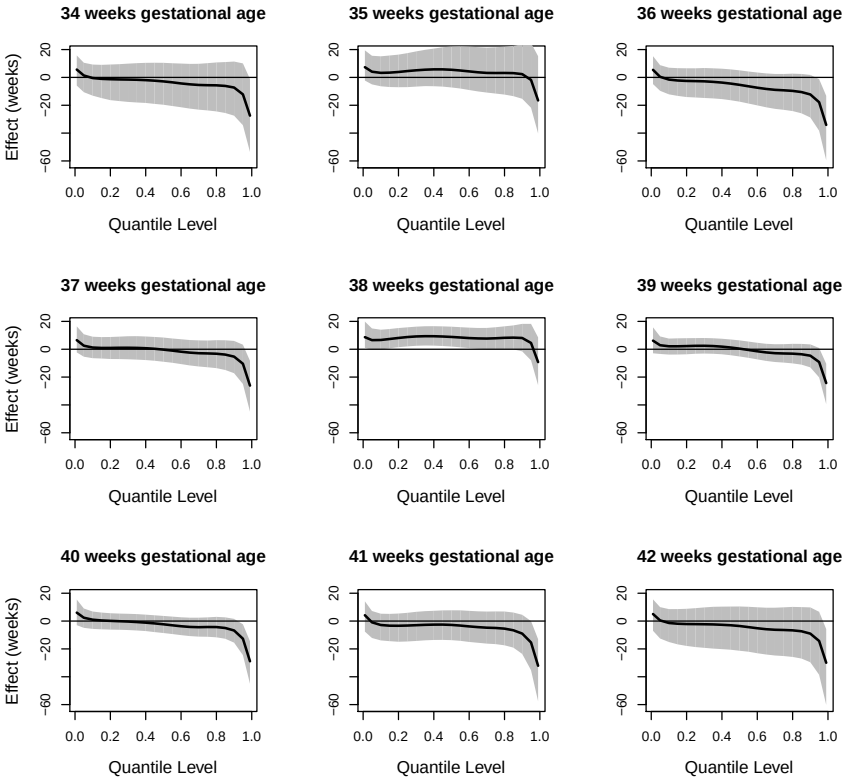

Figure 47. 95% credible limits for the posterior distribution of the effect of the father finishing high school relative to not finishing high school on birth weight for gestational ages 34-42 weeks.

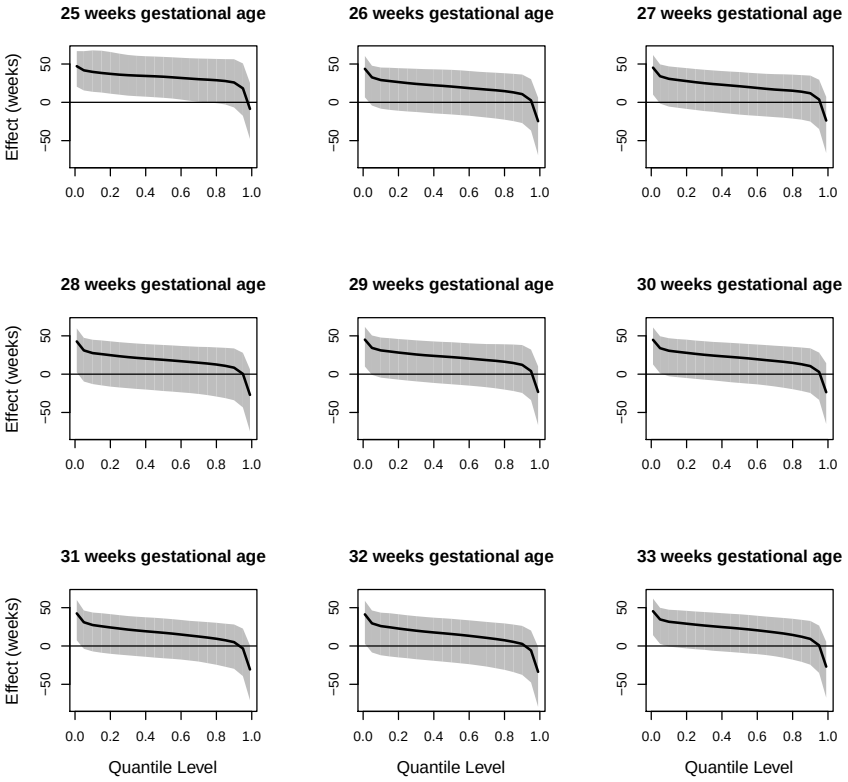

Figure 48. 95% credible limits for the posterior distribution of the effect of the father finishing education above high school relative to not finishing high school on birth weight for gestational ages 25-33 weeks.

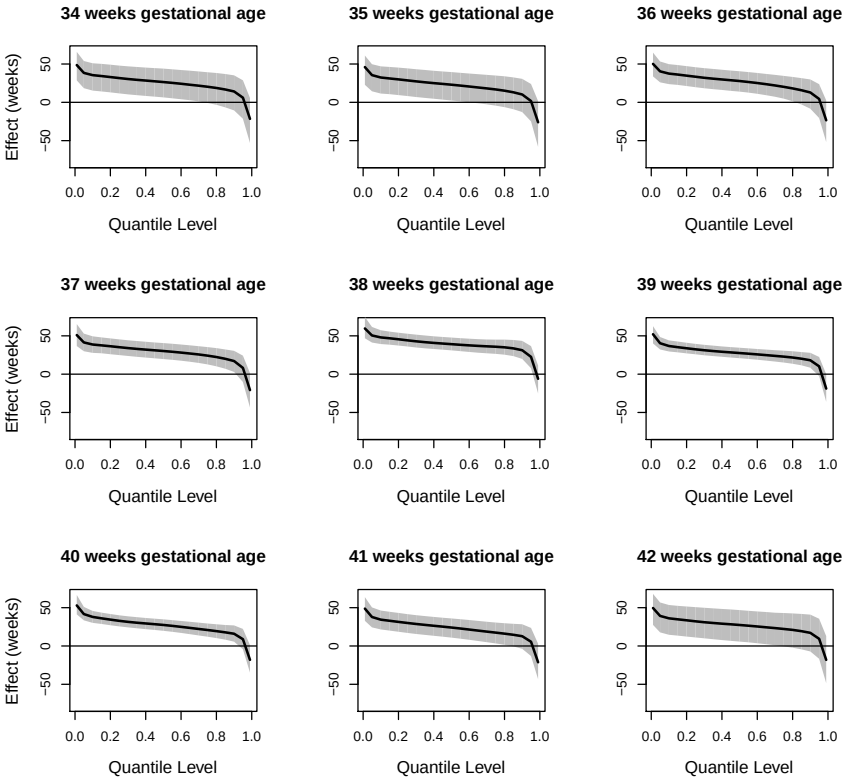

Figure 49. 95% credible limits for the posterior distribution of the effect of the father finishing education above high school relative to not finishing high school on birth weight for gestational ages 34-42 weeks.

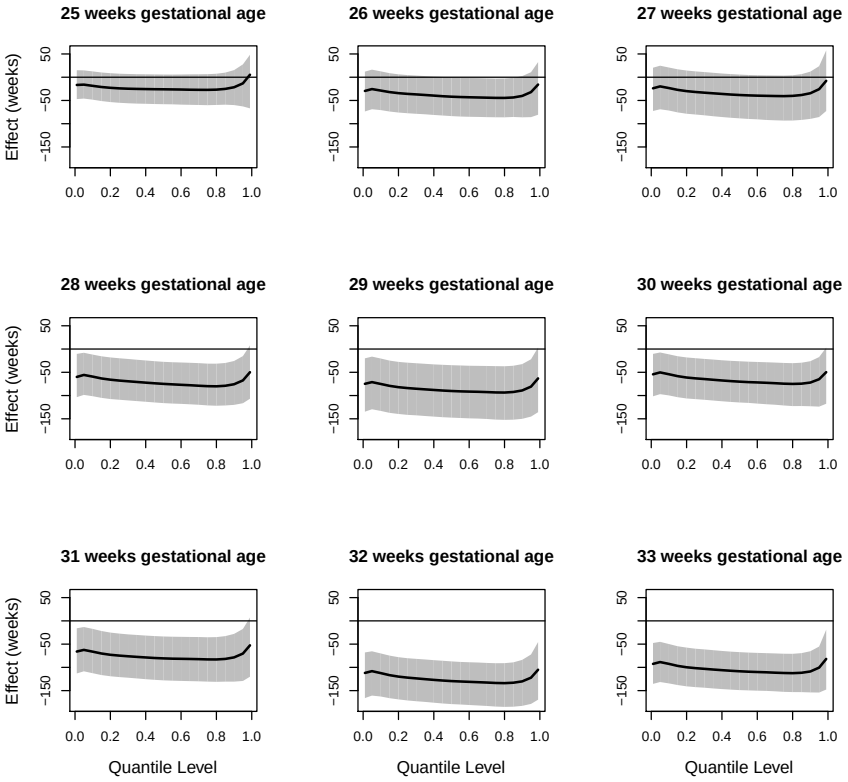

Figure 50. 95% credible limits for the posterior distribution of the effect of maternal black non-Hispanic ethnicity relative to white non-Hispanic ethnicity on birth weight for gestational ages 25-33 weeks.

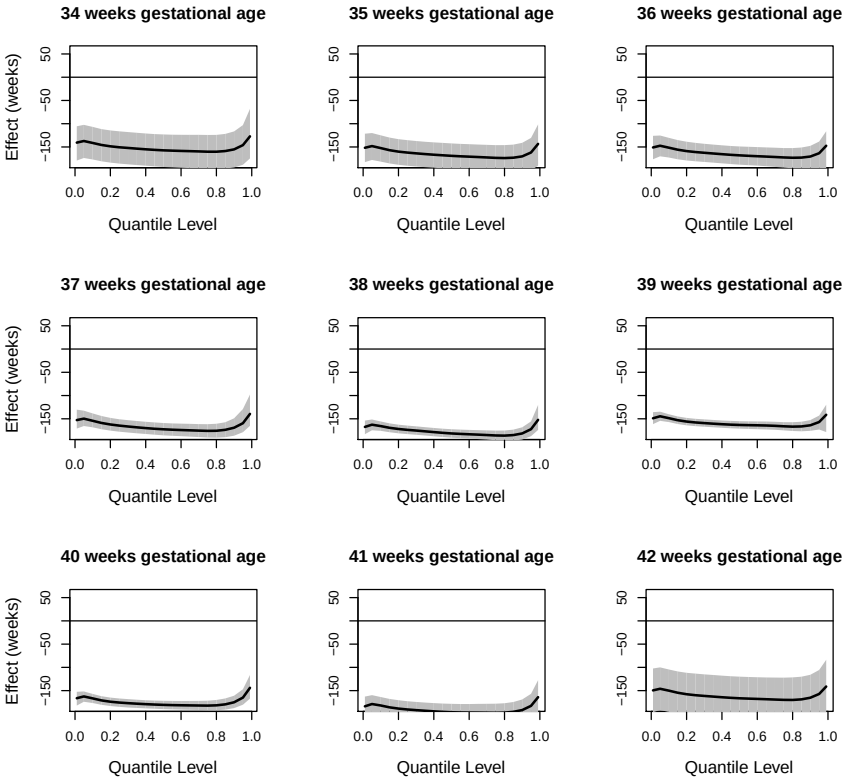

Figure 51. 95% credible limits for the posterior distribution of the effect of maternal black non-Hispanic ethnicity relative to white non-Hispanic ethnicity on birth weight for gestational ages 34-42 weeks.

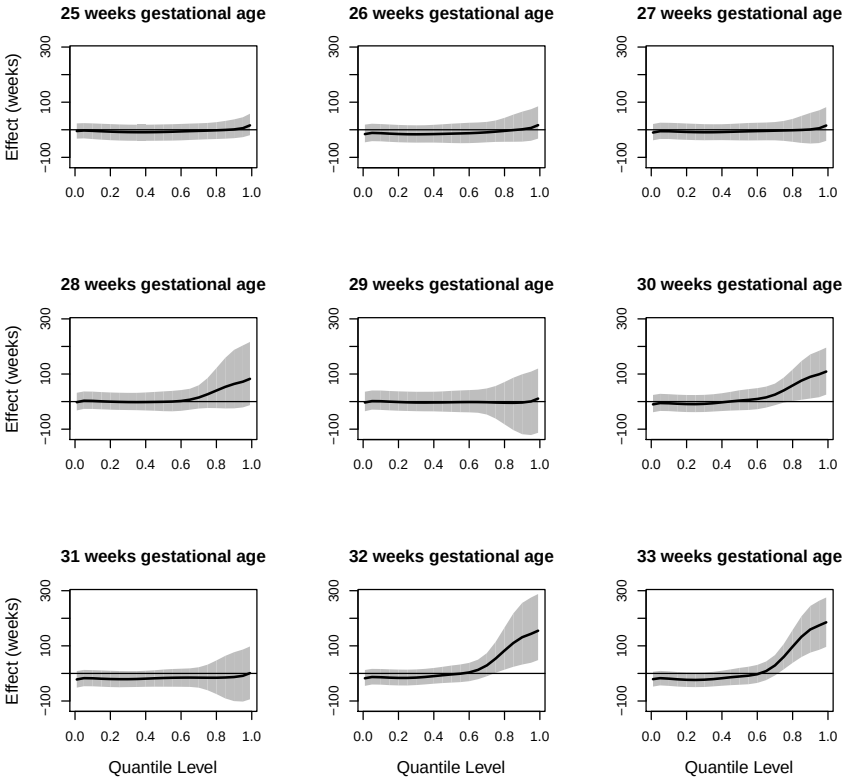

Figure 52. 95% credible limits for the posterior distribution of the effect of maternal Hispanic ethnicity relative to white non-Hispanic ethnicity on birth weight for gestational ages 25-33 weeks.

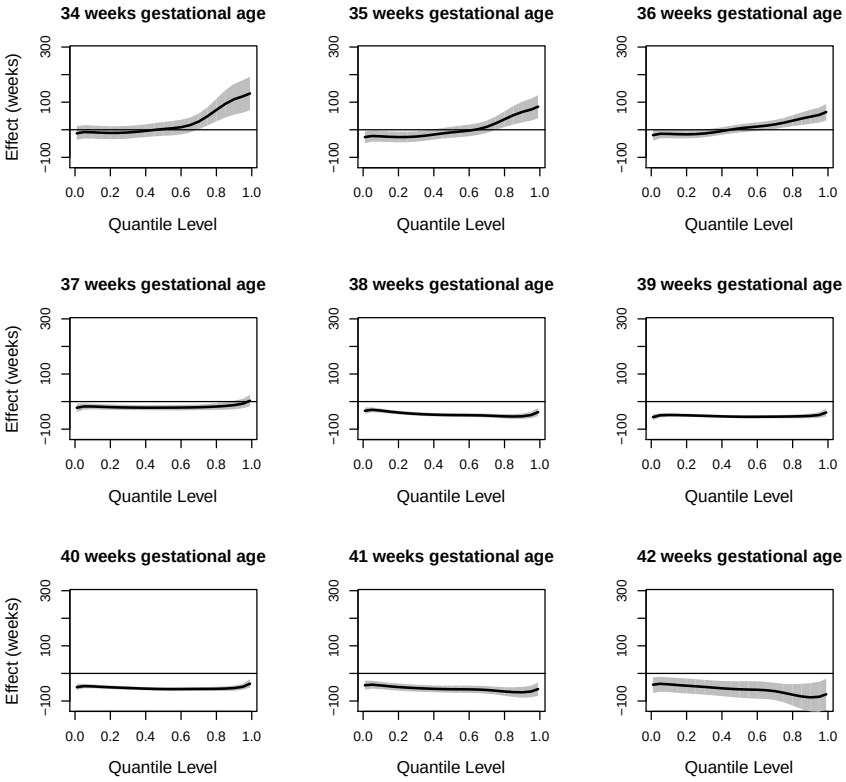

Figure 53. 95% credible limits for the posterior distribution of the effect of maternal Hispanic ethnicity relative to white non-Hispanic ethnicity on birth weight for gestational ages 34-42 weeks.

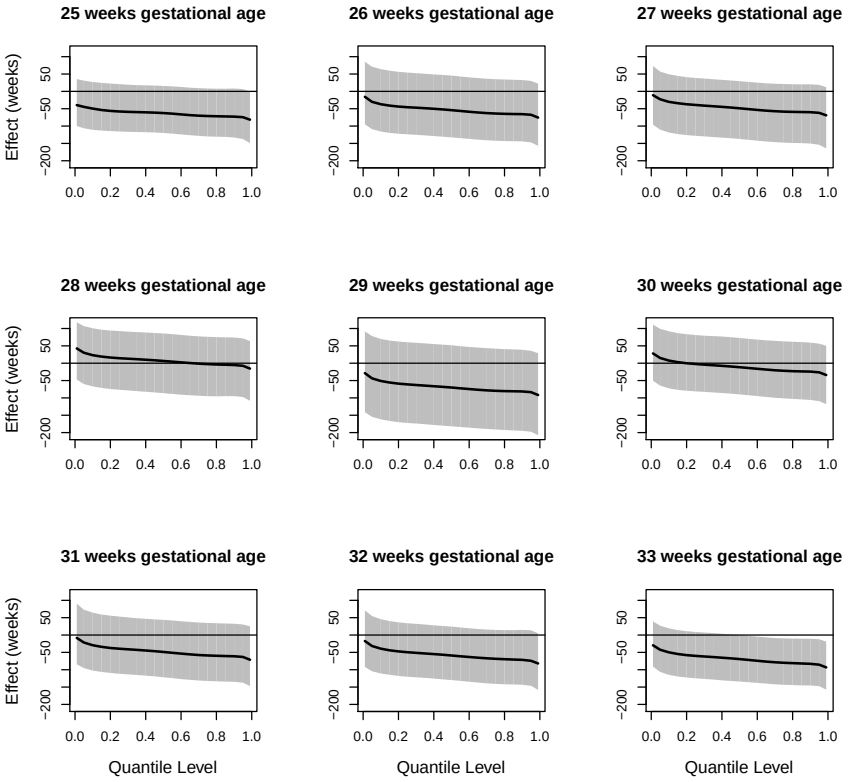

Figure 54. 95% credible limits for the posterior distribution of the effect of maternal other ethnicity relative to white non-Hispanic ethnicity on birth weight for gestational ages 25-33 weeks.

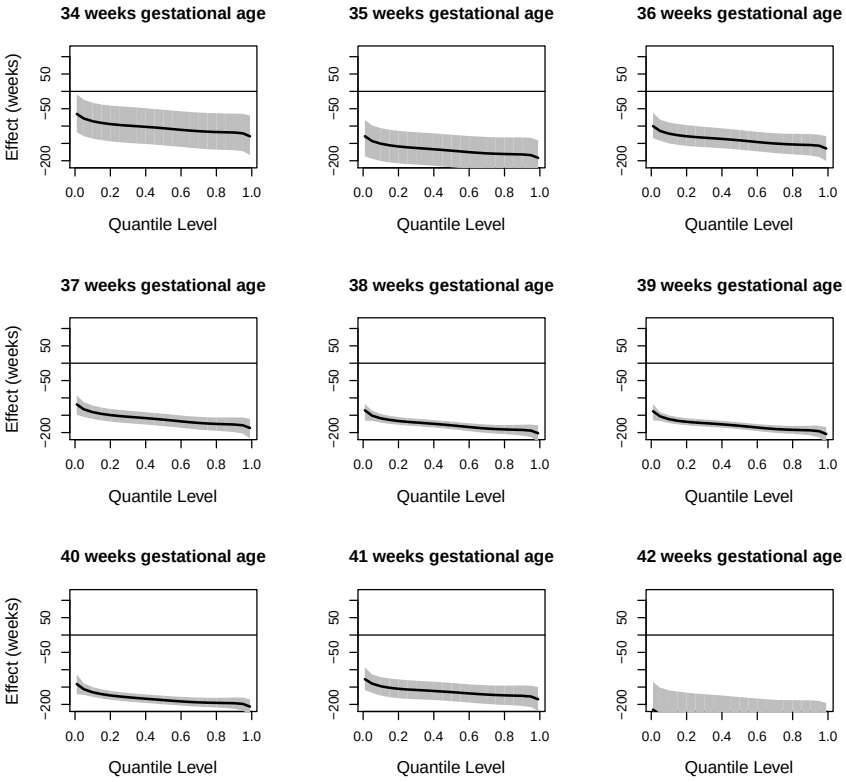

Figure 55. 95% credible limits for the posterior distribution of the effect of maternal other ethnicity relative to white non-Hispanic ethnicity on birth weight for gestational ages 34-42 weeks.

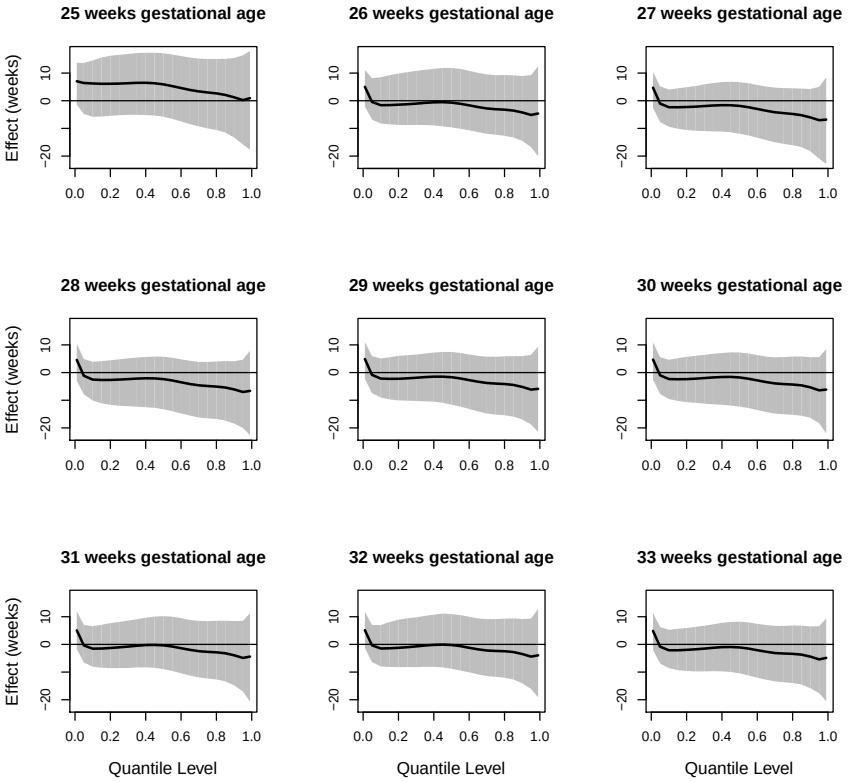

Figure 56. 95% credible limits for the posterior distribution of the effect of a one unit increase in first trimester ozone exposure on birth weight for gestational ages 25-33 weeks. All ozone values were linearly transformed into [-1,1], so a one-unit increase can be roughly thought of as an increase from low levels to middle levels of exposure, or middle to high.

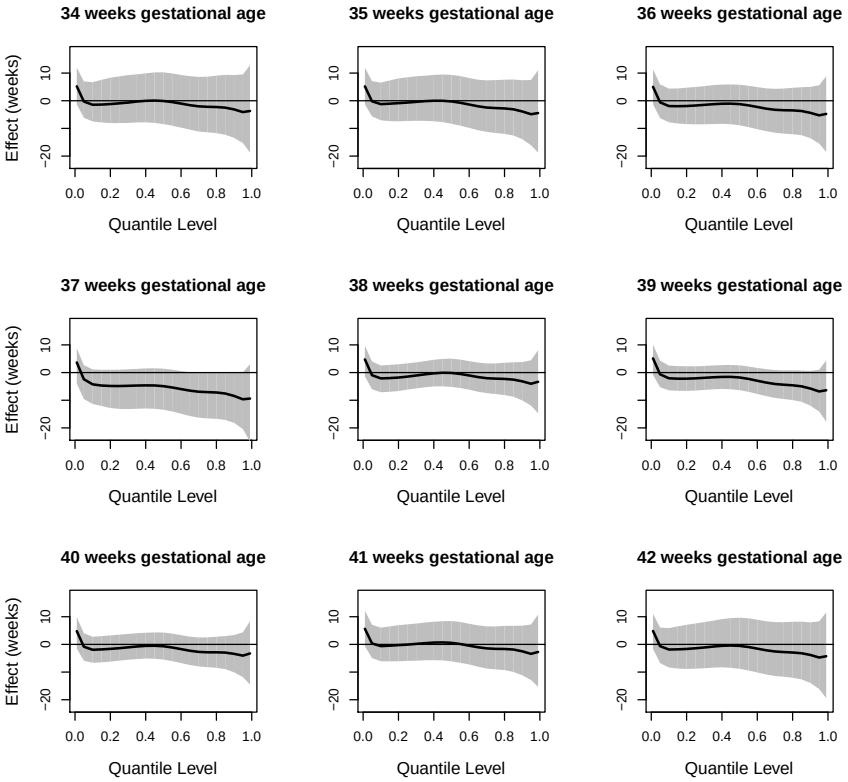

Figure 57. 95% credible limits for the posterior distribution of the effect of a one unit increase in first trimester ozone exposure on birth weight for gestational ages 34-42 weeks. All ozone values were linearly transformed into [-1,1], so a one-unit increase can be roughly thought of as an increase from low levels to middle levels of exposure, or middle to high.

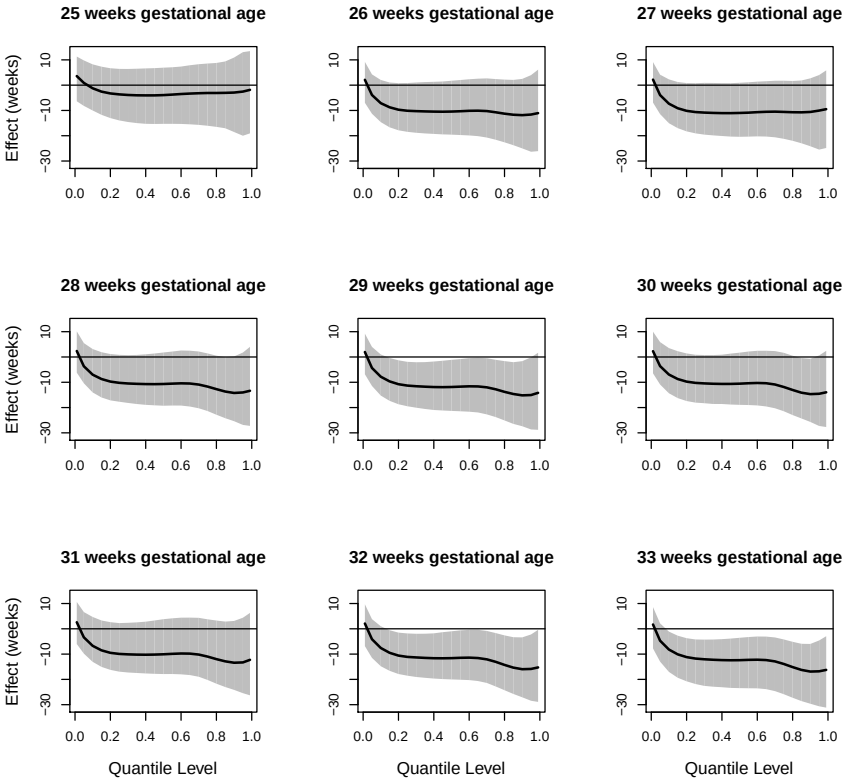

Figure 58. 95% credible limits for the posterior distribution of the effect of a one unit increase in second trimester ozone exposure on birth weight for gestational ages 25-33 weeks. All ozone values were linearly transformed into [-1,1], so a one-unit increase can be roughly thought of as an increase from low levels to middle levels of exposure, or middle to high.

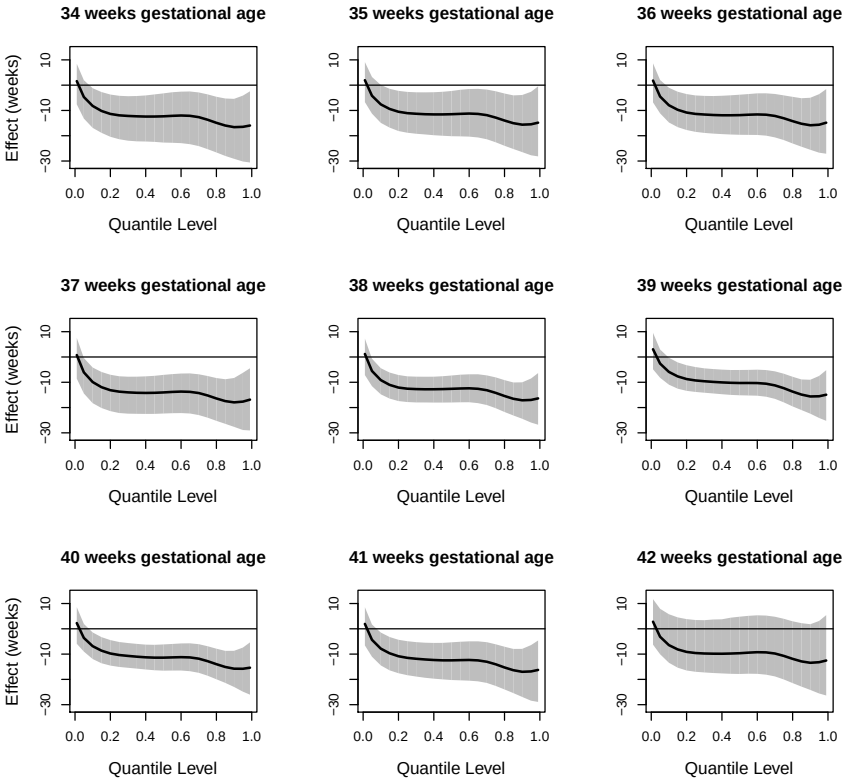

Figure 59. 95% credible limits for the posterior distribution of the effect of a one unit increase in second trimester ozone exposure on birth weight for gestational ages 34-42 weeks. All ozone values were linearly transformed into [-1,1], so a one-unit increase can be roughly thought of as an increase from low levels to middle levels of exposure, or middle to high.